

EMIW2022
Çeşme | Turkey



Near Surface EM Technologies: Archaeological and Environmental Applications

İrfan AKCA

Ankara University, Faculty of Engineering, Department of Geophysical Eng. Gölbaşı Ankara, Türkiye
iakca@eng.ankara.edu.tr

1. Introduction

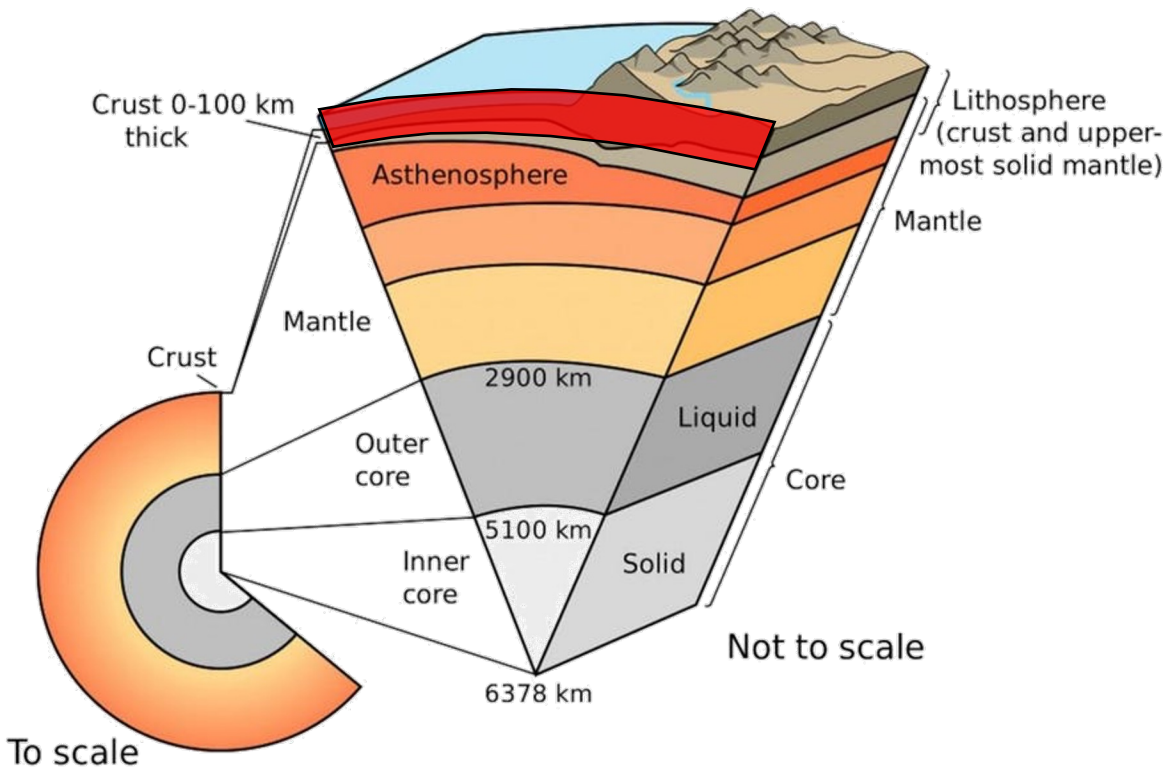
2. Near surface EM methods and their applications

3. Archaeological Prospection

4. Developments in GPR measurement systems

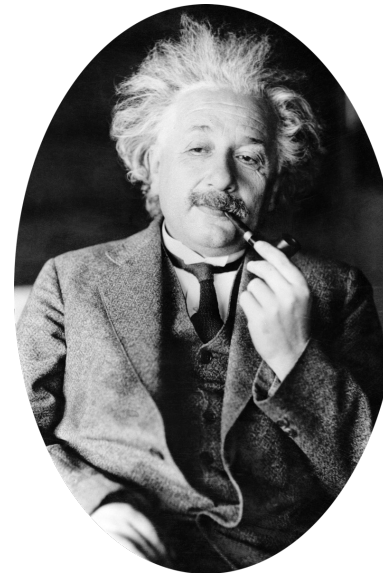
- **Examples**

5. Conclusions



Credit: USGS

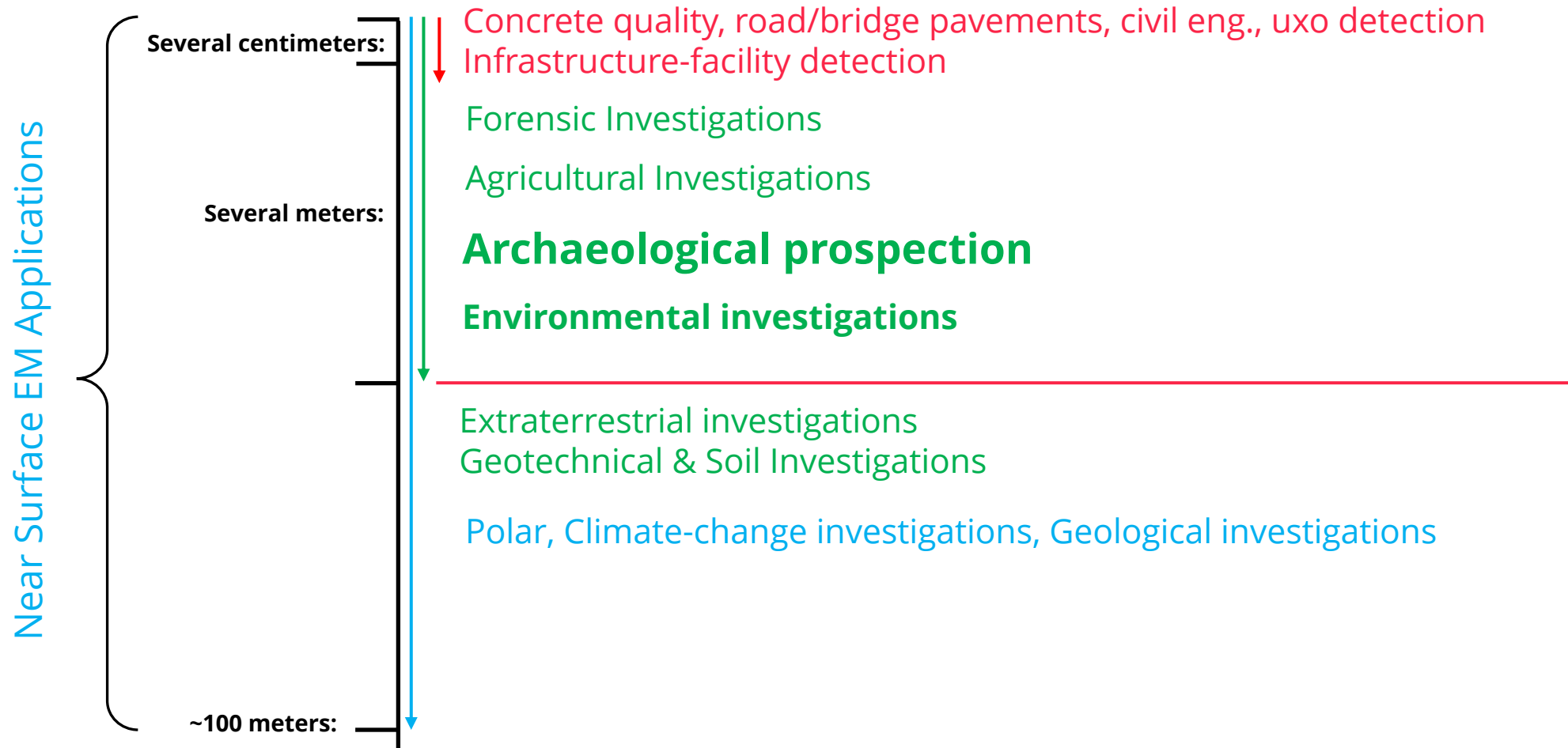
«Near-surface geophysics is generally defined as the use of geophysical methods to investigate the upper few meters to hundreds of meters of the Earth's crust.»



The word «Near» is relative

- [Everett \(2012\)](#) defines it <1km
- and in this presentation it is limited to ~10 meters

(very very near surface)



Archaeological Places In Turkey



Troy



Hittite Empire (1650-1200 BC)



Ephesus, Miletos, Milet, Didyma



Çatalhöyük (7000BC) (first bread wheat)



Göbeklitepe (~10000BC)

- An archaeological excavation can be conducted only once and destroy the experiment site irreversibly.

• Euro... on

• «...SC... destru...
poss... (2017)

• Geo... gation

• I...

• C R

• E

• Grave



the

inve

on-



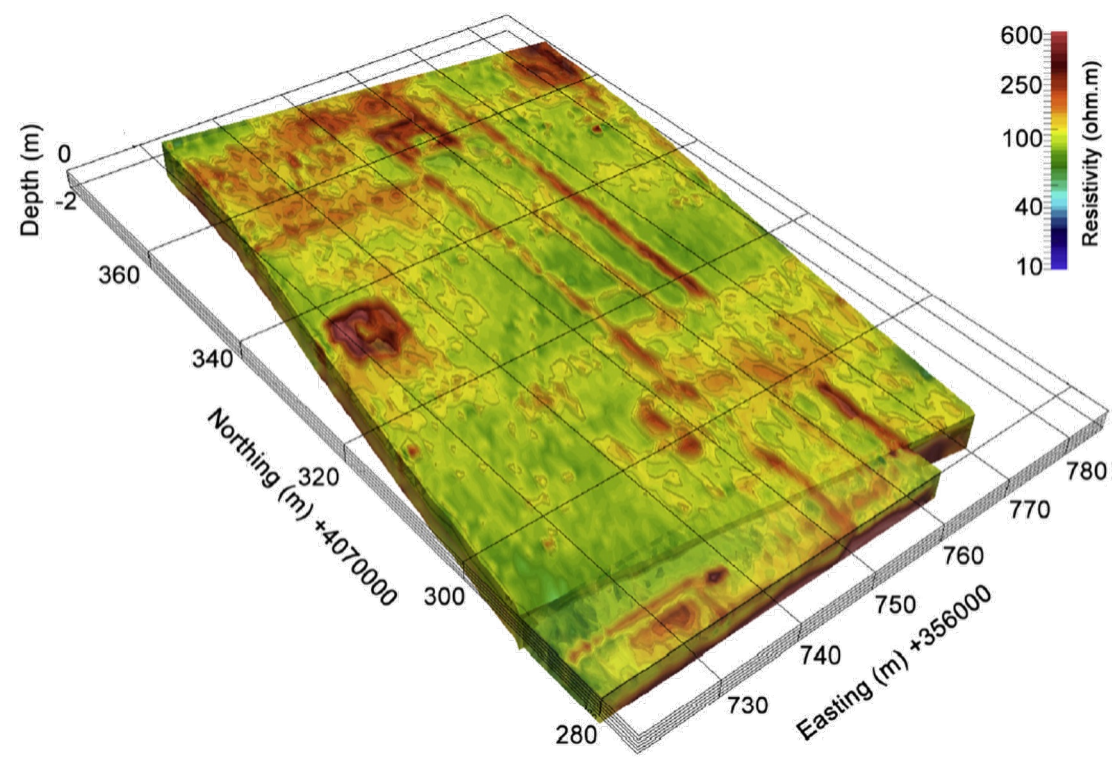
Excavations



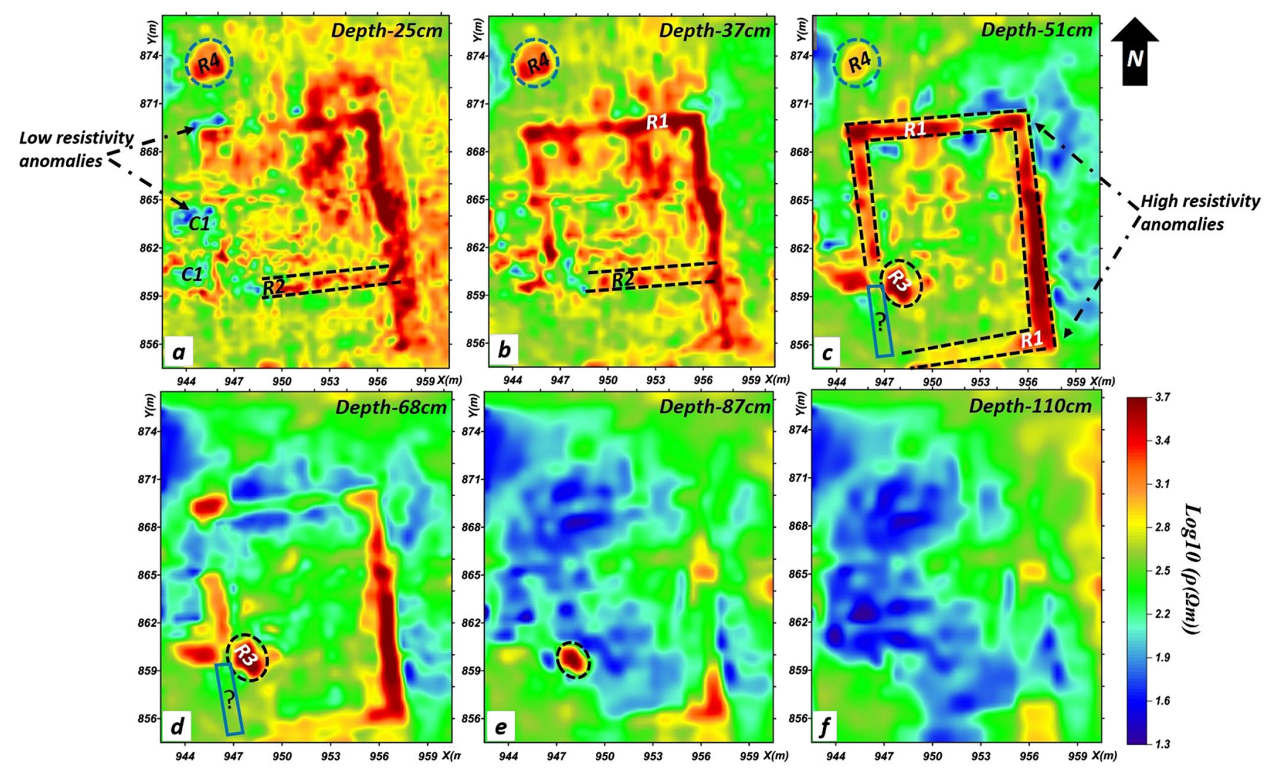
struc

su

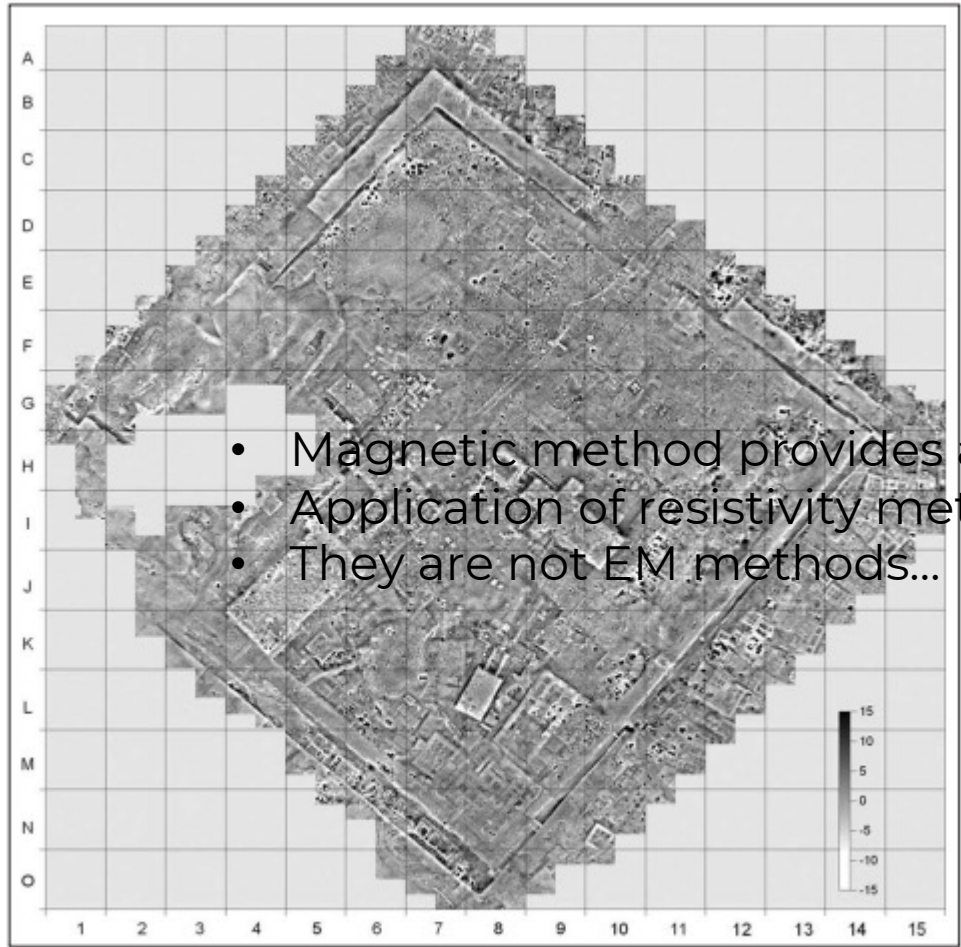
Akca et al. (2017)



(Akca et al. 2017)



(Al Saadi et al. 2018)



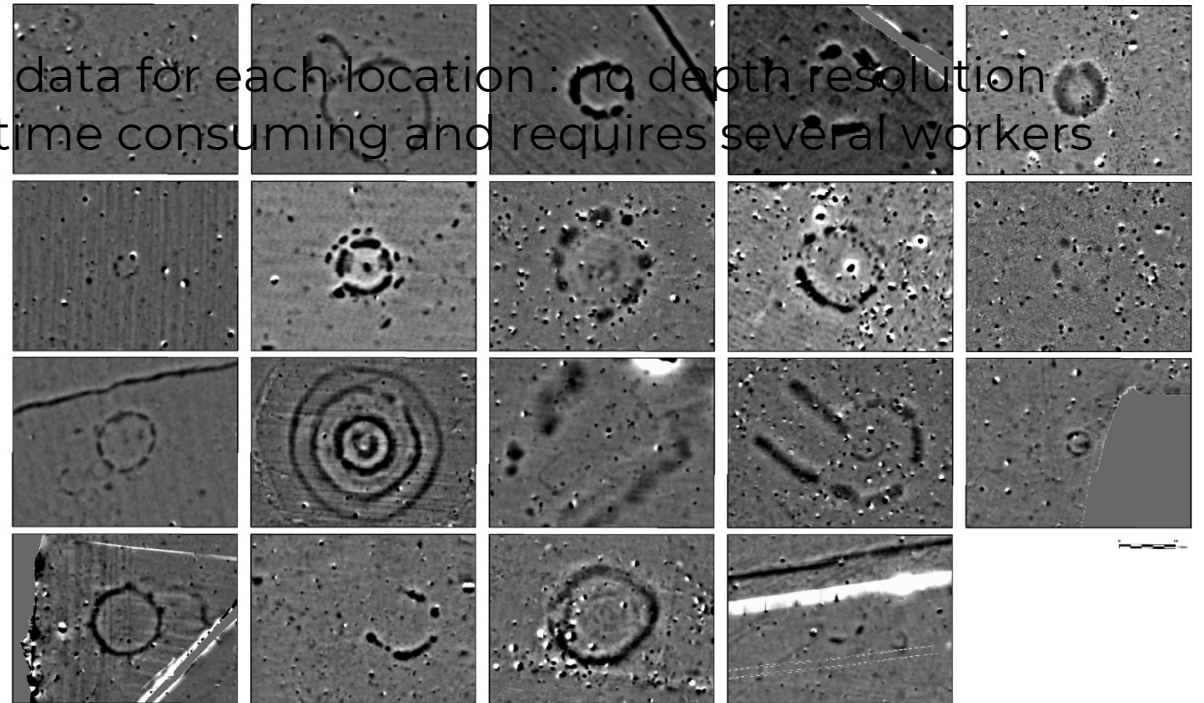
- Magnetic method provides a single data for each location : no depth resolution
- Application of resistivity method is time consuming and requires several workers
- They are not EM methods...

Fig. 2. Magnetic map of Tell el-Balamun. Fluxgate Geoscan Research FM36 and FM256 gradiometers. Sampling grid 0.25 by 0.50 m, interpolated to 0.25 m by 0.25 m. Dynamics -9 nT (white)/+16 nT (black). Grid lines every 40 m (Processing T. Herbich)

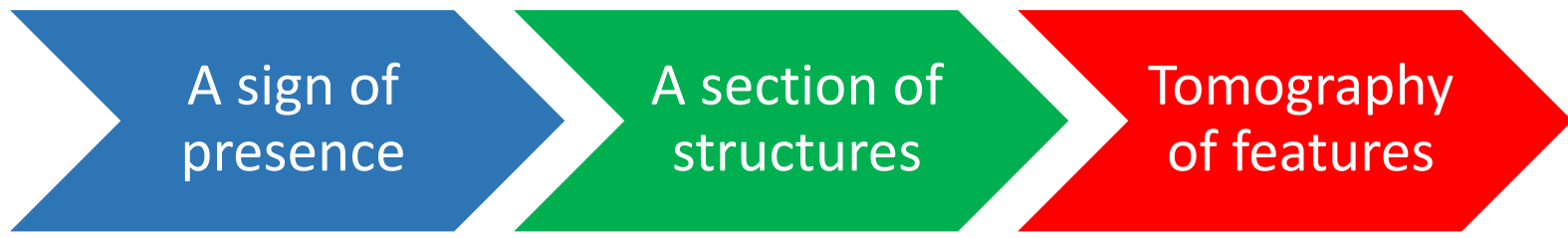
(Herbich and Spencer, 2008)



Trinks et al., 2012



Gaffney, et al., 2018



>1940s

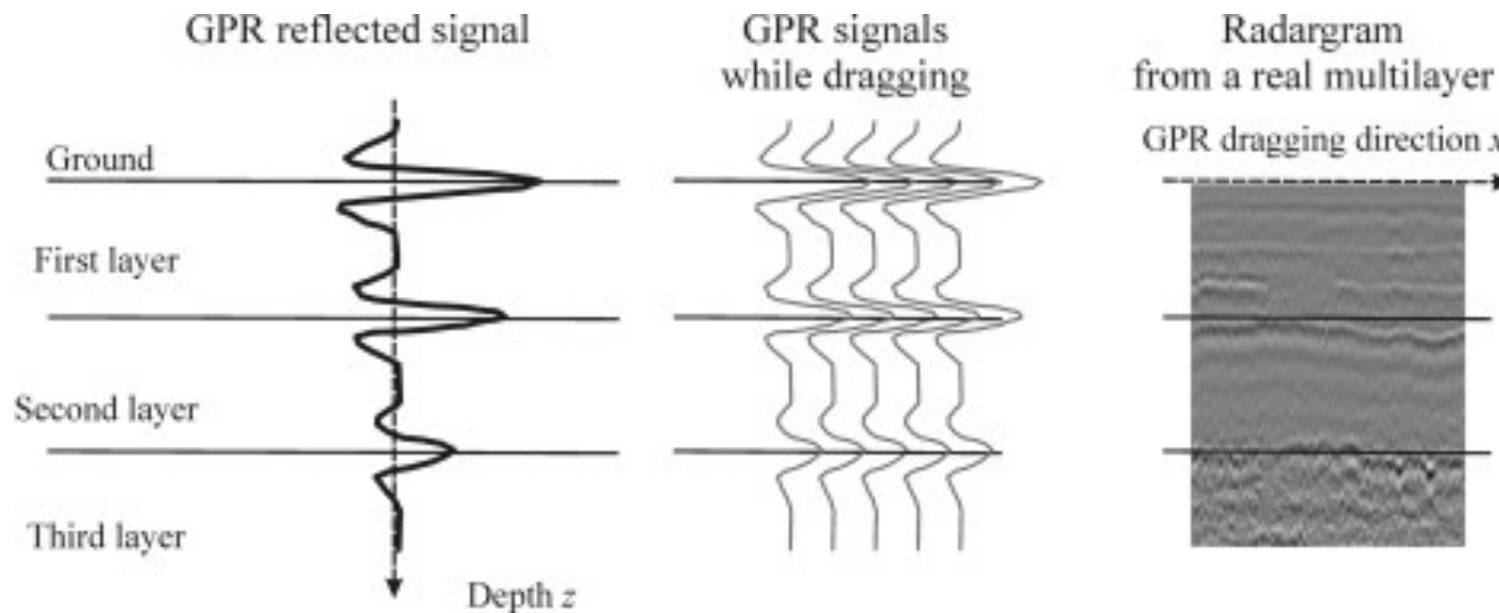
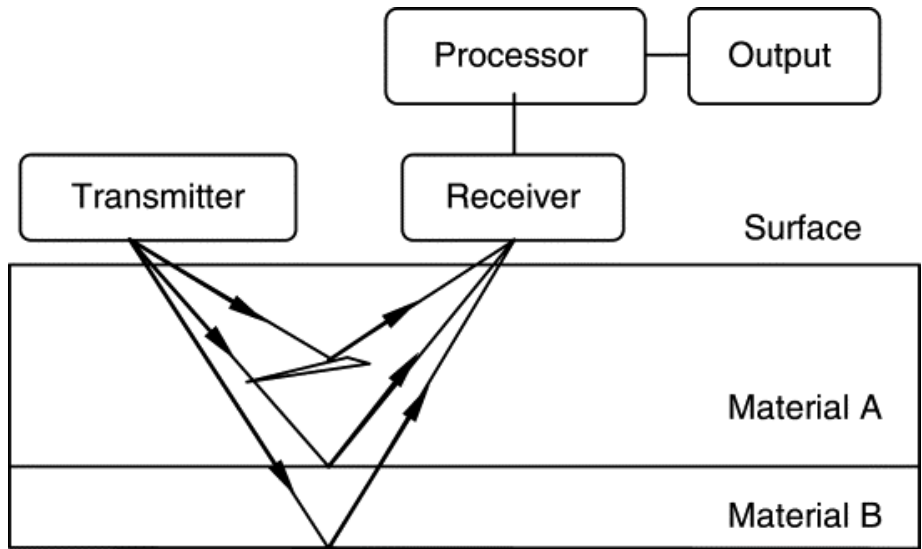
1980s

2000s



- 3S (Becker, 2009)
- Speed
 - Sensitivity
 - Spatial Resolution

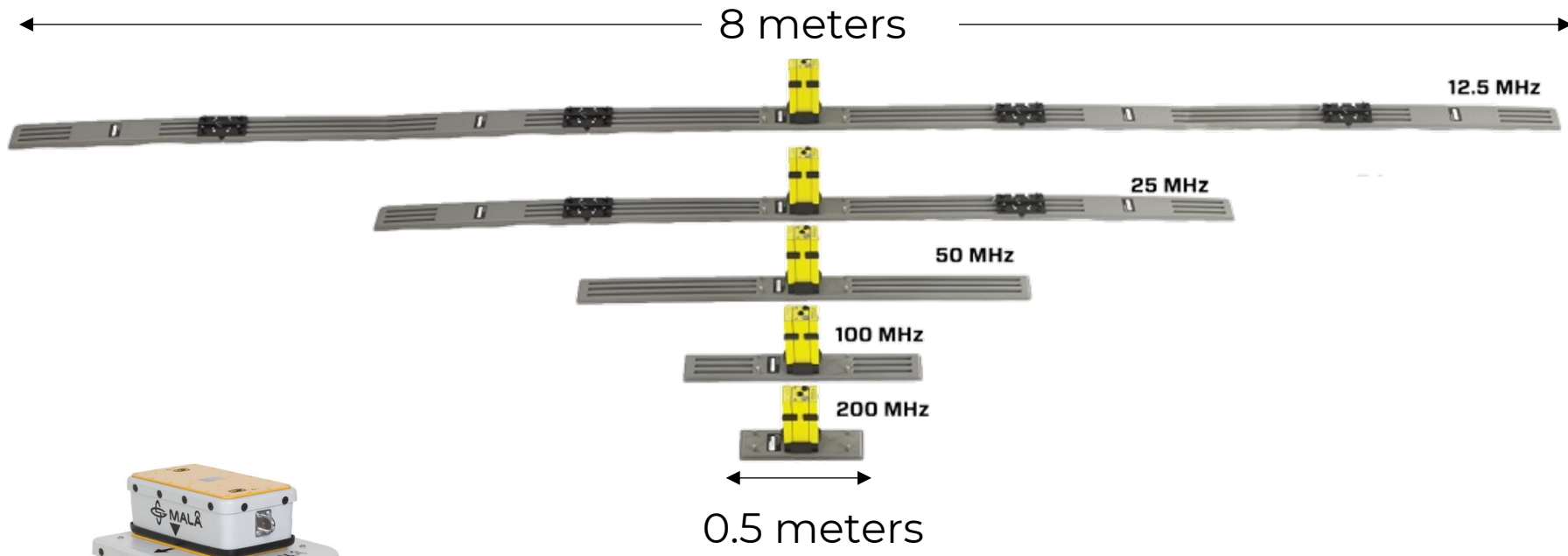
Ground Penetrating Radar (GPR)



(Dong and Ansari, 2011)



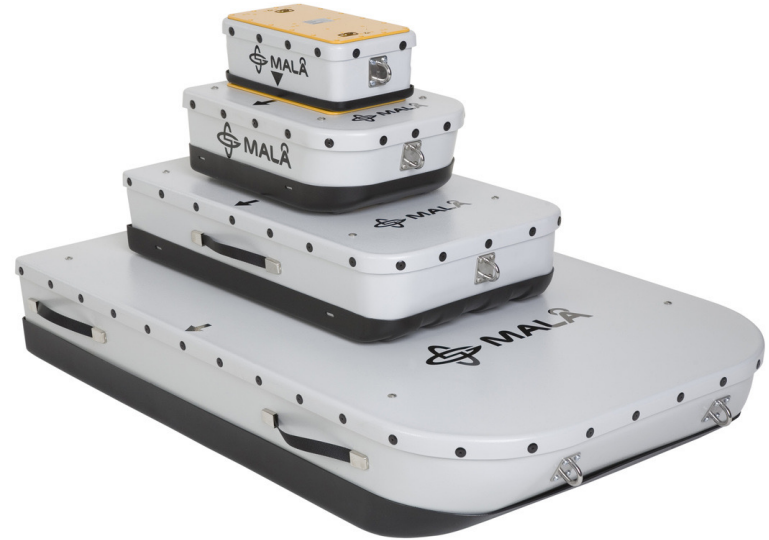
2.7GHz



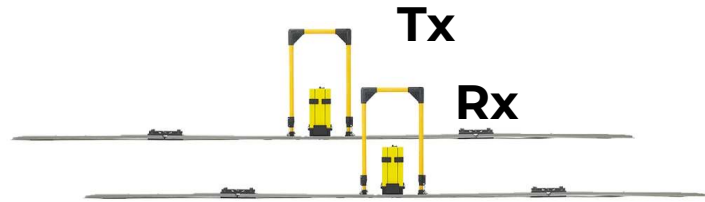
Resolution

Frequency

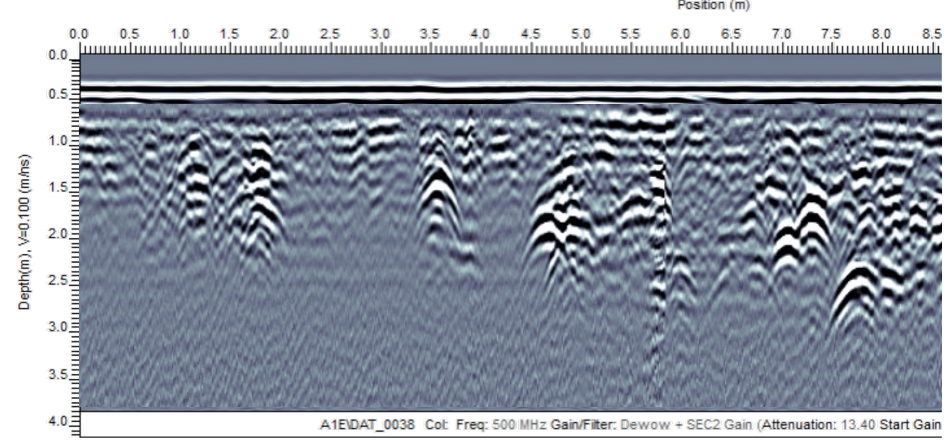
Penetration Depth



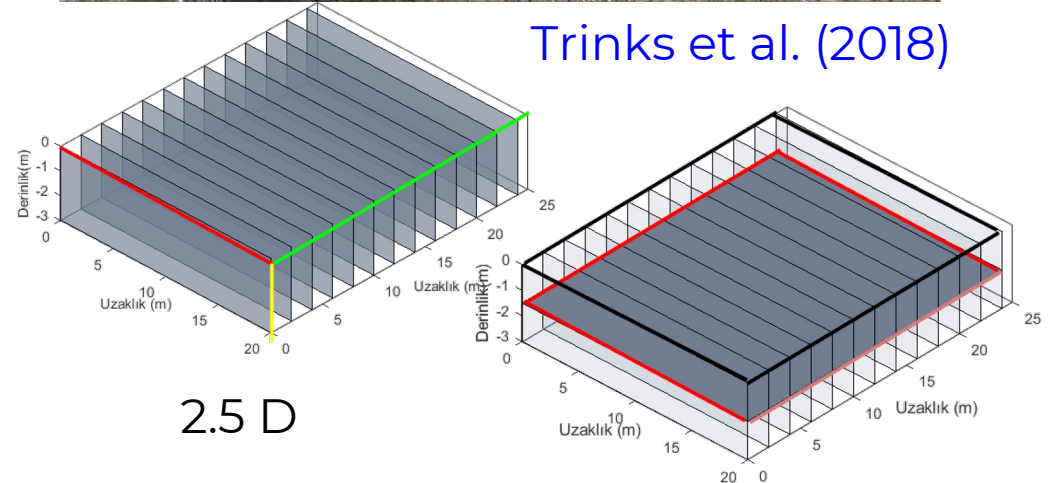
100-800MHz

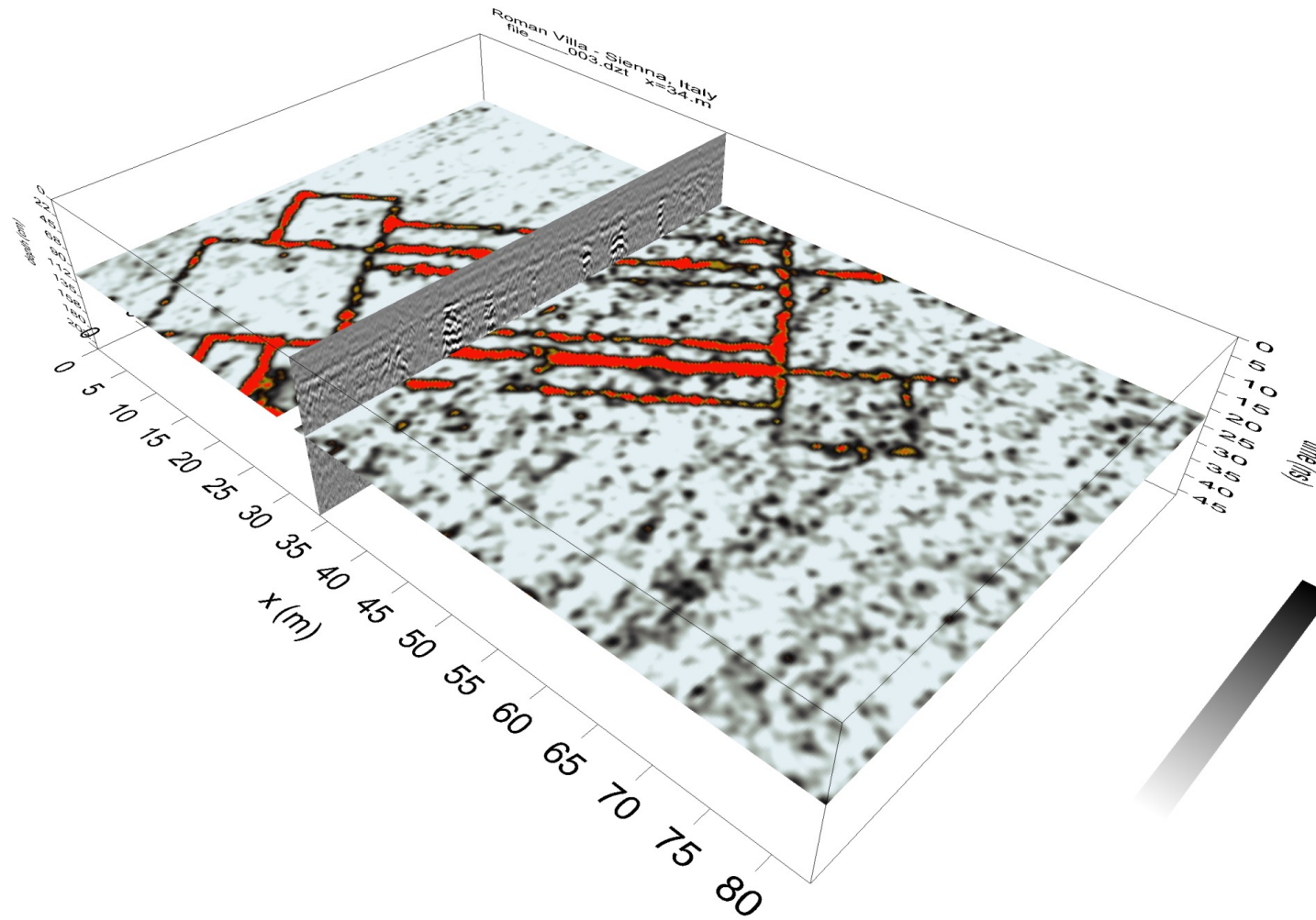


Conyers, L. (2013) introduces GPR into archaeological prospection in 1970s.
Reading: (Annan 2009, Goodman and Piro ,2013)



Trinks et al. (2018)





Depth ~1m Roman villa near Sienna, Italy ([Campana et al. 2006](#))

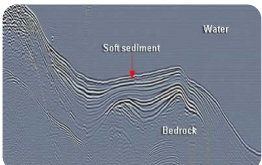
- 1. Survey speed
- 2. Measurement Sensitivity
- 3. Spatial Sampling
- 4. New Application Areas



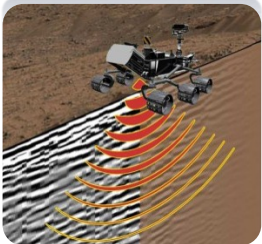
Specialized CARTS with GPS integrated



Multi-channel GPR Systems &| Antenna Arrays



Marine & Submarine Applications



RIMFAX GPR on MARS



Airborne GPR : Drone or UAV based

Survey speed - Spatial Sampling

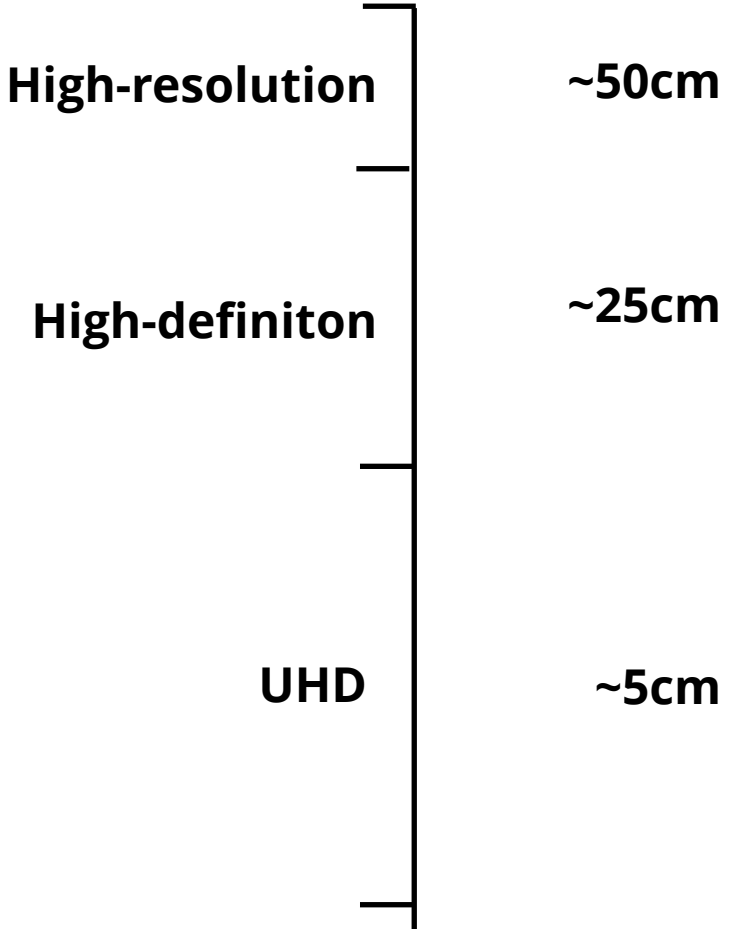
Cross-line spacing

In-line spacing

(trace spacing)

$$\Delta x \leq v_{\min} / 4f_{\max}$$

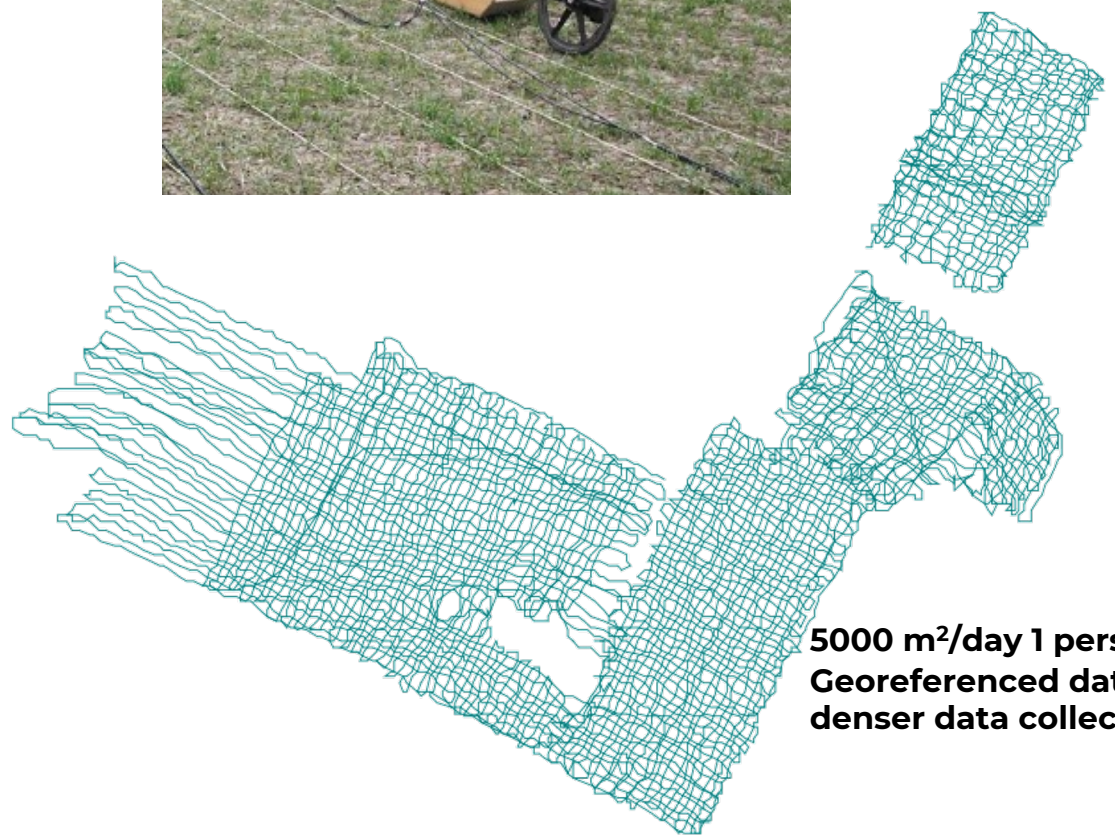
Grasmueck, Weger and Horstmeyer (2003,2005)



Frequency (MHz)	Trace Spacing (cm)
100	10-20
250	5-10
500	2-5

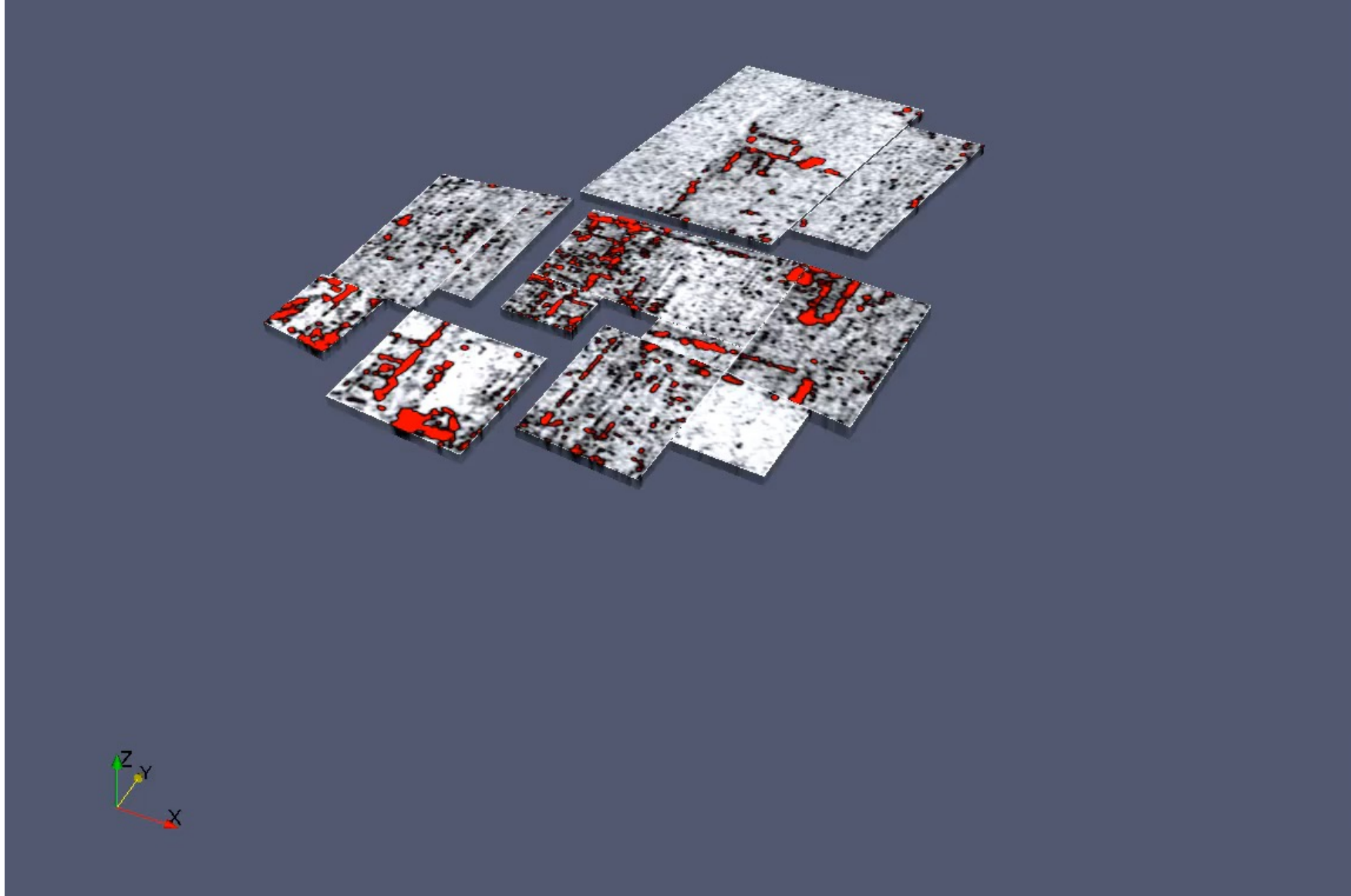


Specialized CARTS with GPS integrated



5000 m²/day 1 person
Georeferenced data,
denser data collection





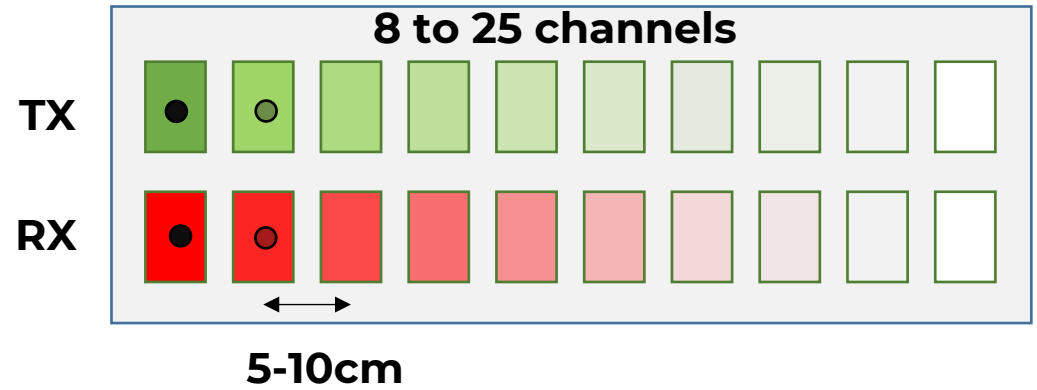


- 1 Radar control unit
- 2 Survey wheel with encoder
- 3 400 MHz antenna
- 4 Collapsible frame
- 5 Quick release, foam-filled wheels



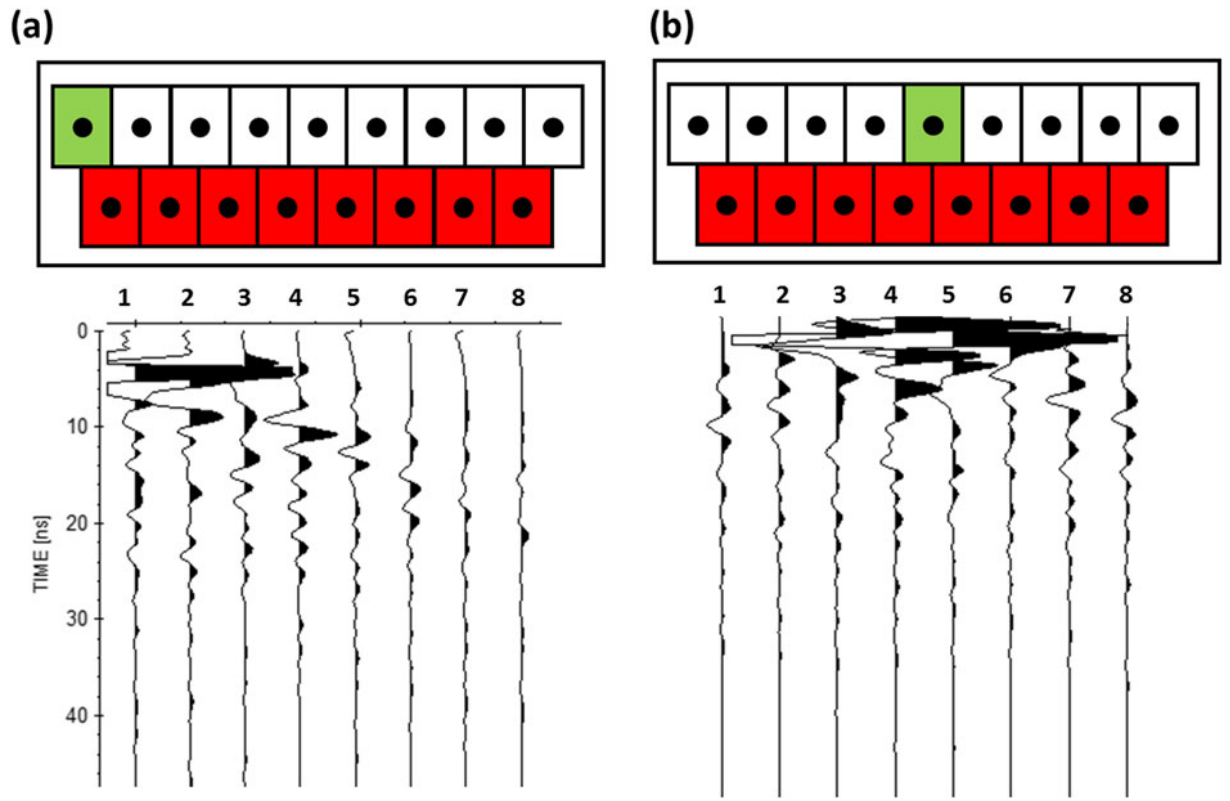


Multi-static



See [Berard and Maillol \(2008\)](#), [Booth, Linford, Clark, and Murray, \(2008\)](#) for studies on measurements with different sequences of TX RX pairs.

Multi-offset (3D)





Article

Georeferencing of Multi-Channel GPR—Accuracy and Efficiency of Mapping of Underground Utility Networks

Marta Gabryś * and Łukasz Ortyl

Faculty of Mining Surveying and Environmental Engineering, AGH University of Science and Technology, al. Mickiewicza 30, 30-059 Kraków, Poland; ortyl@agh.edu.pl

* Correspondence: gabrys@agh.edu.pl

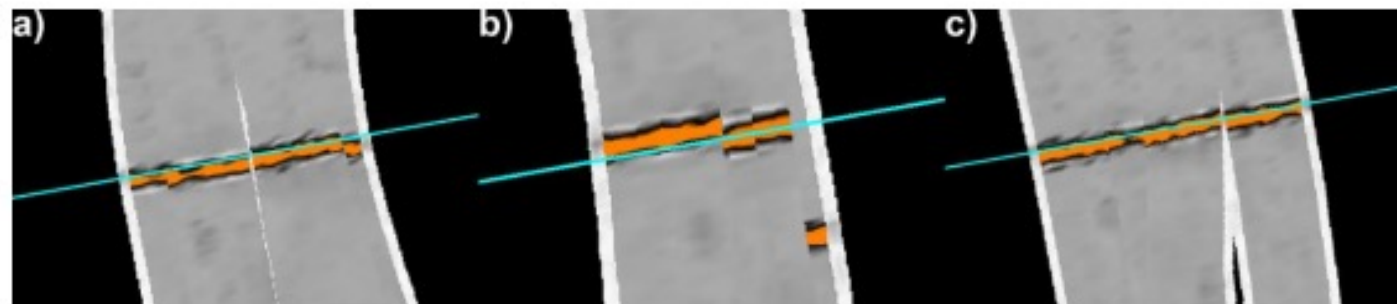


Figure 9. Resulting C-scans for parallel passes positioned with the use of: (a) GPS PPS (b) GPS and (c) the total station—with the scanned drainage grille in the background.

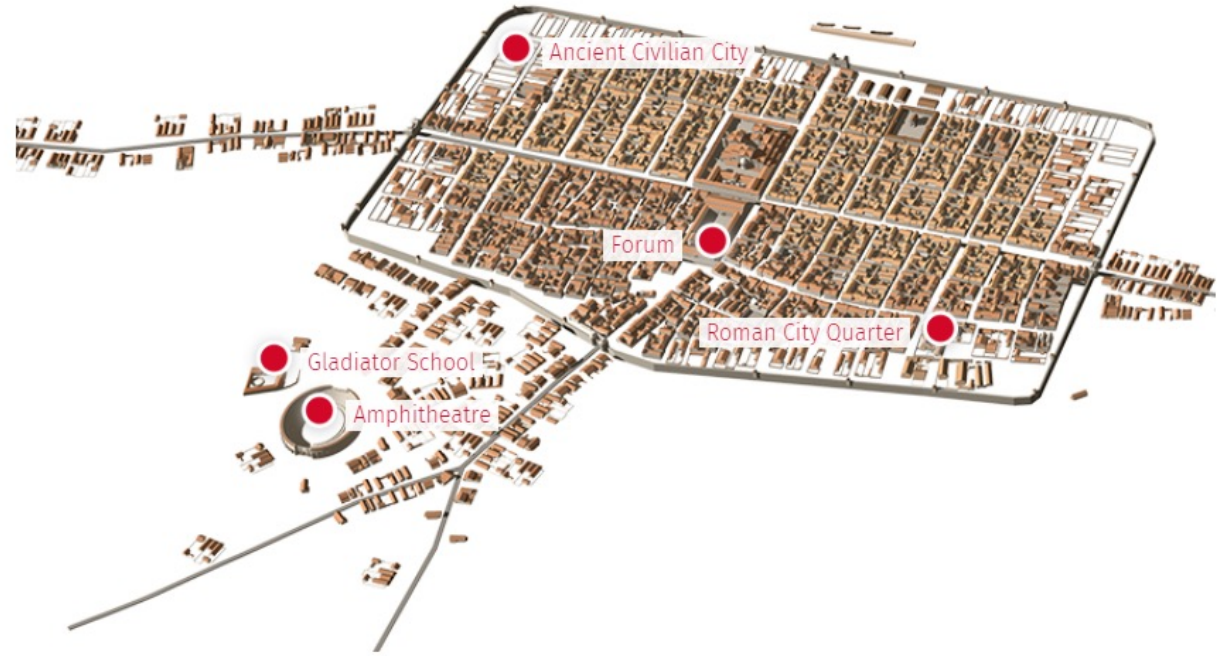
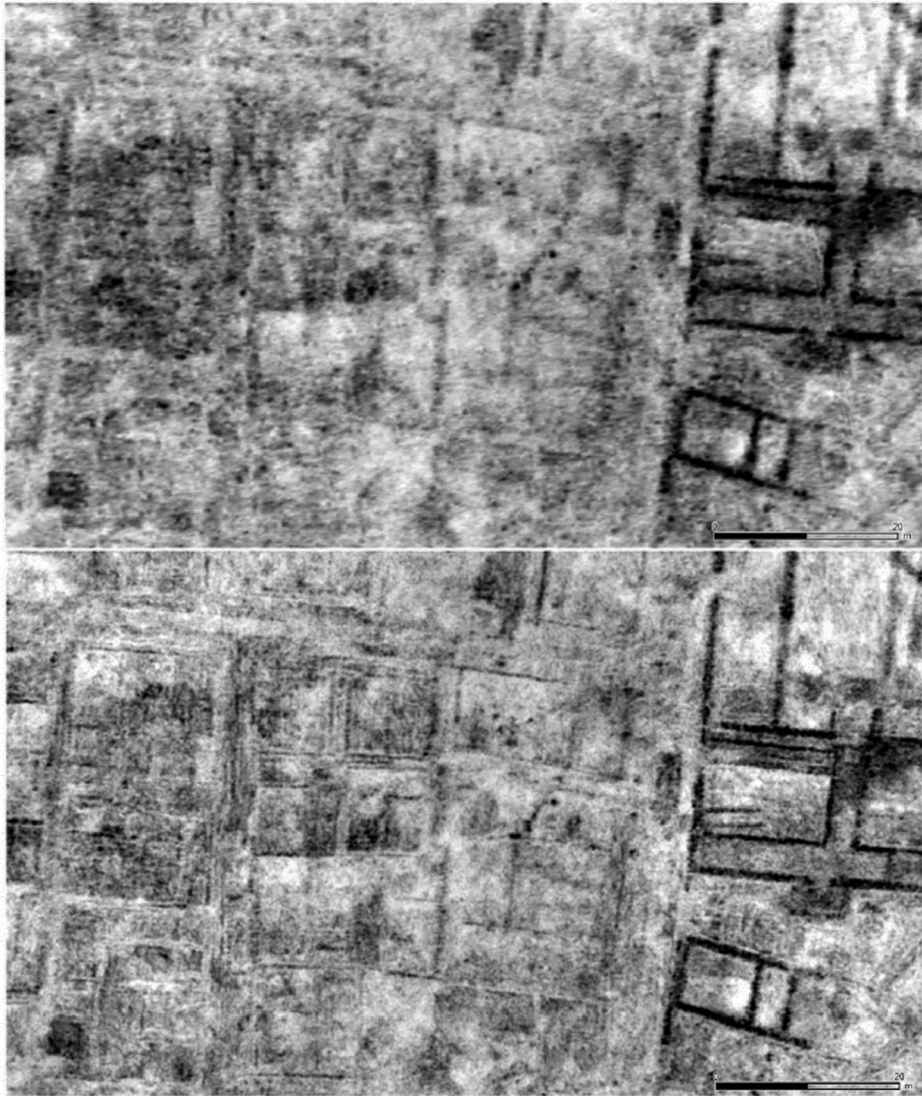


FIGURE 21 Comparison of MIRA data sampled with 48 cm cross-line channel spacing in the Civil town of Carnuntum (top) versus an high fidelity depth-slice image based on data acquired with 8 cm cross-line channel spacing (bottom), permitting detailed architectural data interpretation with much increased reliability. Inline data acquisition sample spacing has been 4 cm in both cases. The length of the scale-bar is 20 m. Images: Alois Hinterleitner

Trinks et al. (2018)

Article
Archaeological Prospection with Motorised Multichannel Ground-Penetrating Radar Arrays on Snow-Covered Areas in Norway

Manuel Gabler ^{1,*}, Immo Trinks ², Erich Nau ¹, Alois Hinterleitner ³, Knut Paasche ¹, Lars Gustavsen ¹, Monica Kristiansen ¹, Christer Tonning ⁴, Petra Schneidhofer ⁴, Matthias Kucera ² and Wolfgang Neubauer ²



Figure 4. 100 cm thick snow cover at Odberg during the GPR measurements in February 2018. Note the compacted snow caused by the snow crawlers to the right of the yard stick. Photo: Erich Nau.

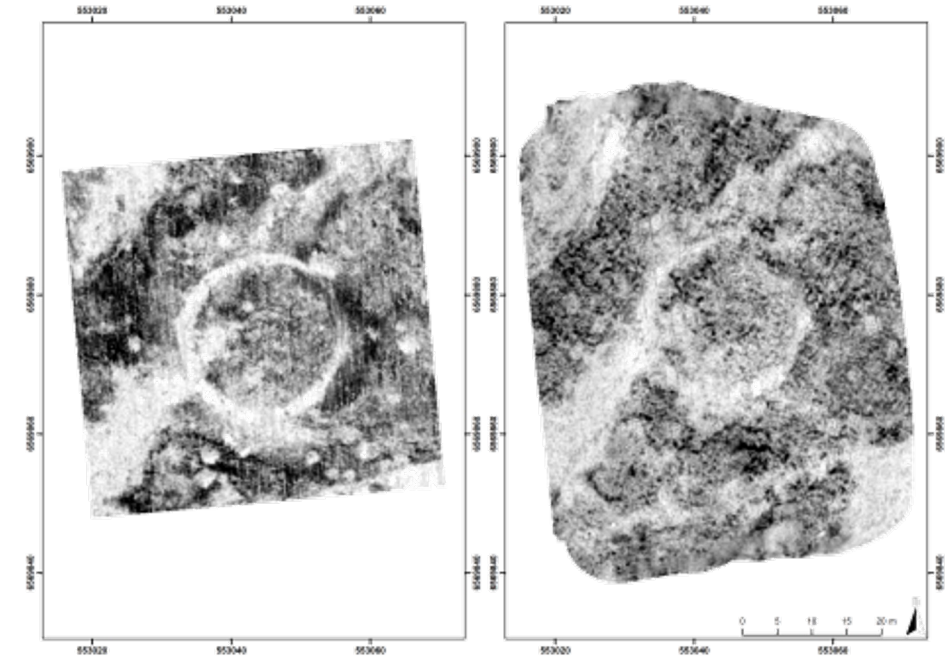
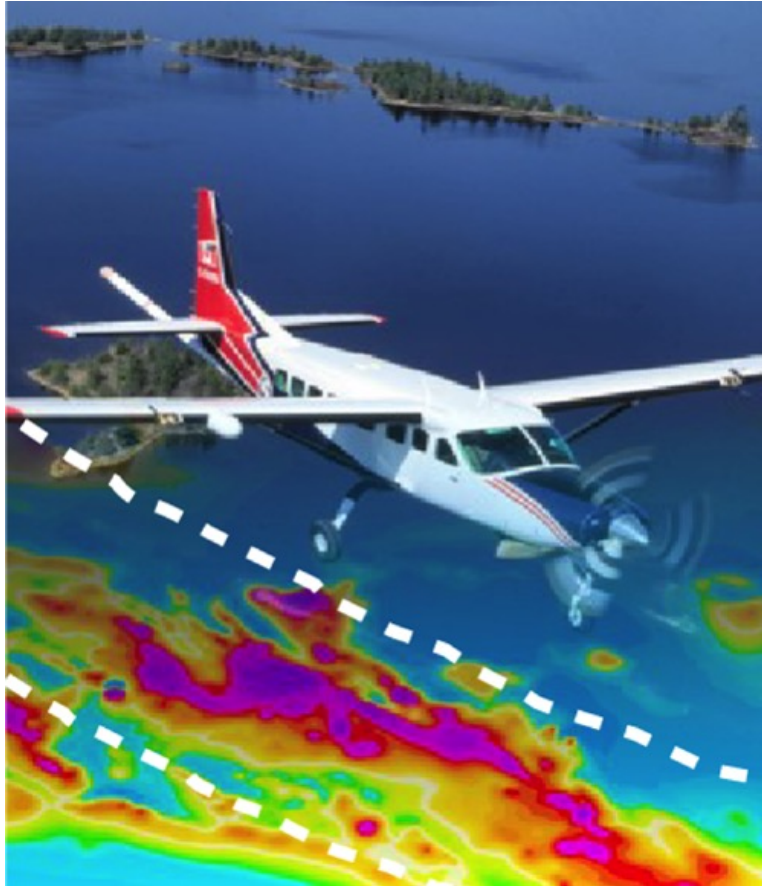
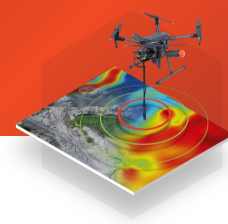


Figure 6. Odberg in Lågendalen: GPR depth-slice comparison with data acquired under snow-free condition (left image) and with snow cover (right image). The remains of an over-ploughed Iron Age burial mound with numerous pits within and in the surrounding area are clearly visible in the left image. The up to one metre thick snow cover resulted in less pronounced GPR anomalies and reduced contrast between the archaeological features and the surrounding soil. The reduced imaging resolution of the measurements on a layer of thick snow are caused by the greater distance and thereby increased GPR antenna footprint. Coordinate system: EUREF89/UTM32N.



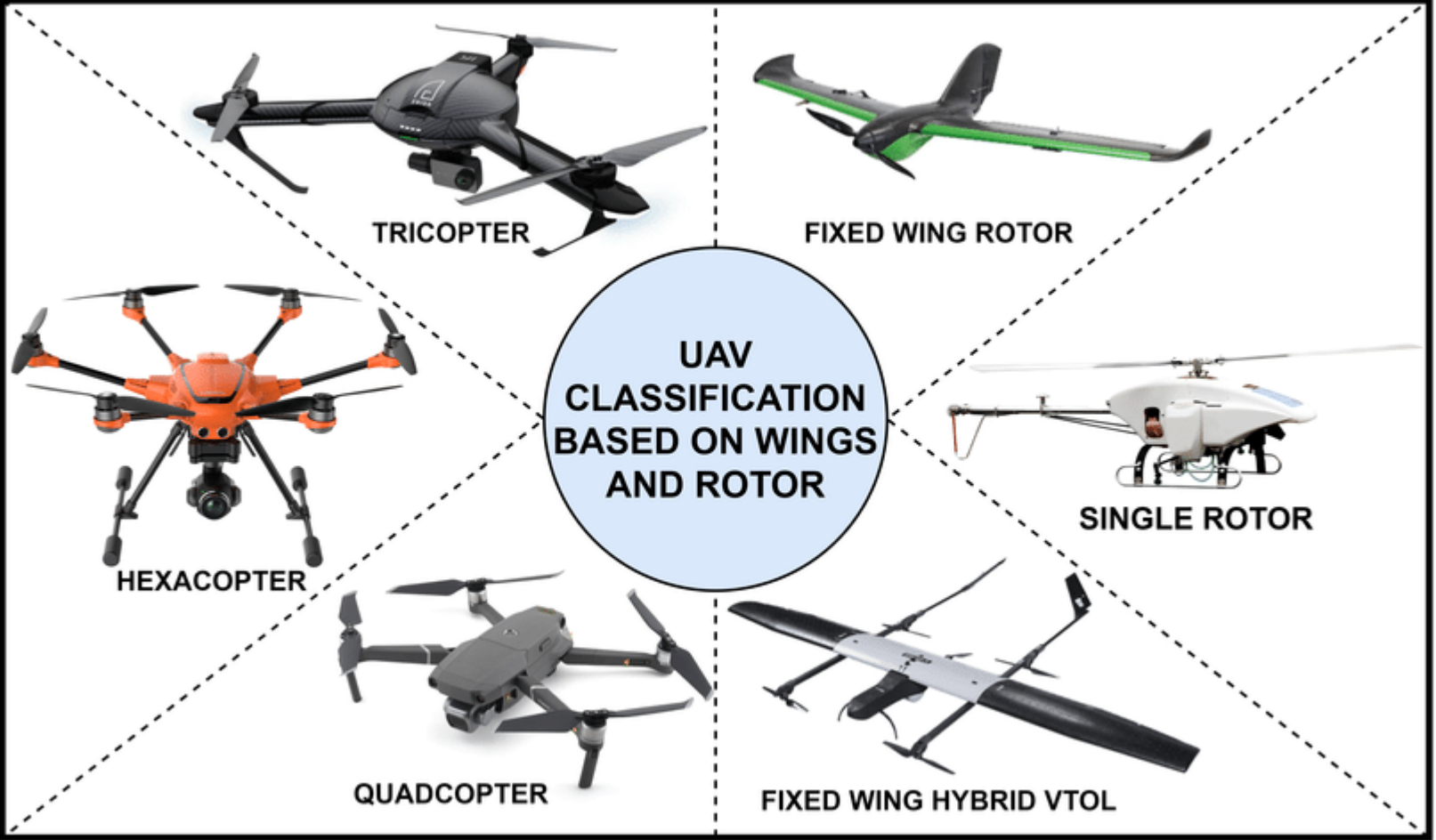
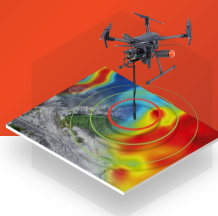
- 1.5ha / hour (15000 sqm - 12000sq.yards)
- Resolution of centimeters
- Handling / processing of huge amount of data
- Transporting vehicles /antennae
- To achieve benefits the terrain should be quite flat and free of obstacles



Credit: USGS



Gravity, Magnetic, Electromagnetic, Radiometric

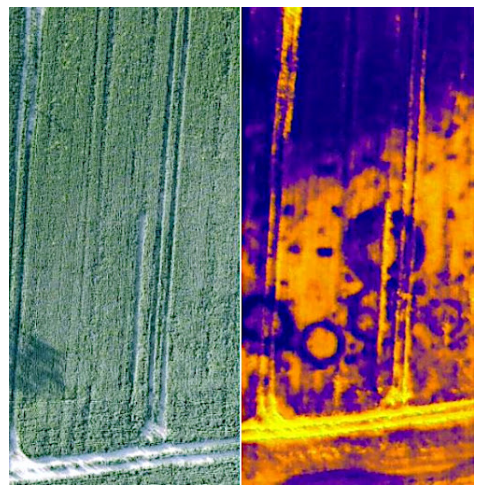
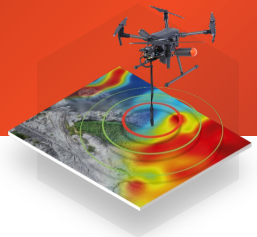


Chamola et al. (2021)

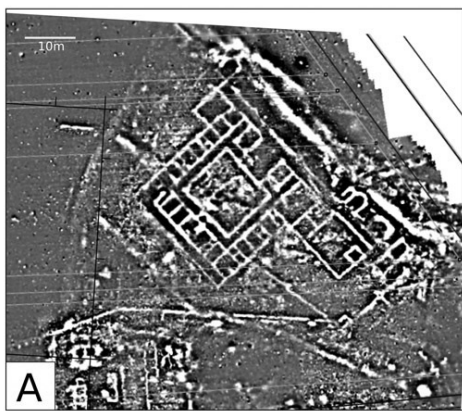


Heavy lift drones, payloads ~100kg

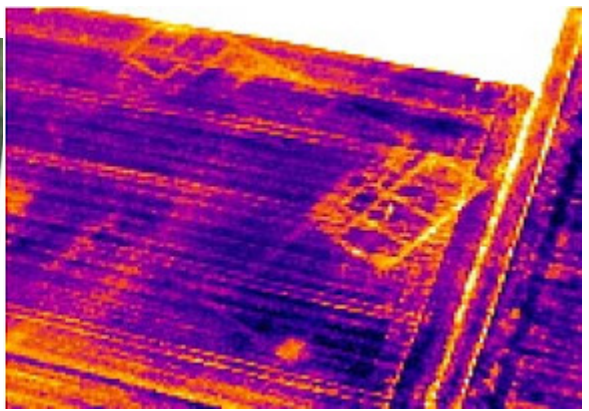
- LIDAR
- Standart RGB cameras
- Spectral / Hyperspectral cameras
- Thermal cameras
- Magnetic sensors
- ...



SENSYS MagDrone R3 magnetometer
Payload is ~1kg



Oedenbourg (France). (Gavazzi et al. 2021)



(Wells, J., 2020)



Figure 6: Octocopter. The MTOW is 25 kg. The max payload is 10 kg @ 25 min endurance

Stoll, et al., (2019)

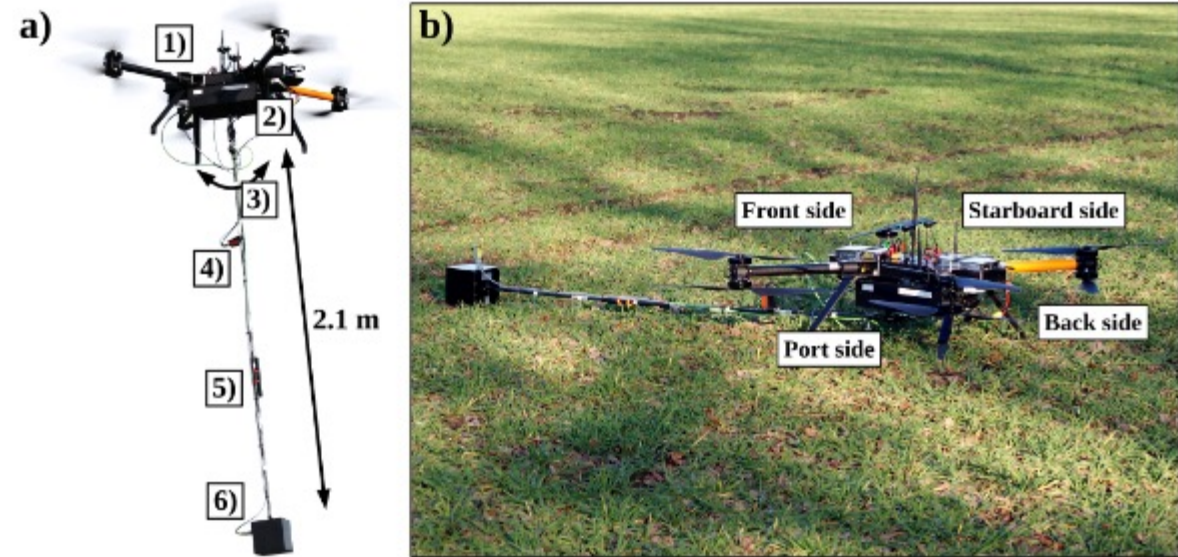









Figure 1. Illustration of the utilized UAS. (a): The Mobile Geophysical Technologies UAS (during operation) composed of a X825 octocopter from Aerialis (1), a compactified Metronix ADU-08e logging device (2), a rigid rod made of carbon fiber (3), a Xsens MTi-G-710 IMU (4), a Bartington Mag-13MSL70 3-axis fluxgate sensor (5) and a Metronix SHFT-02e induction coil triple (6). (b): The UAS with mounted instruments ready for takeoff. Highlighted are the preferential directions of the UAV

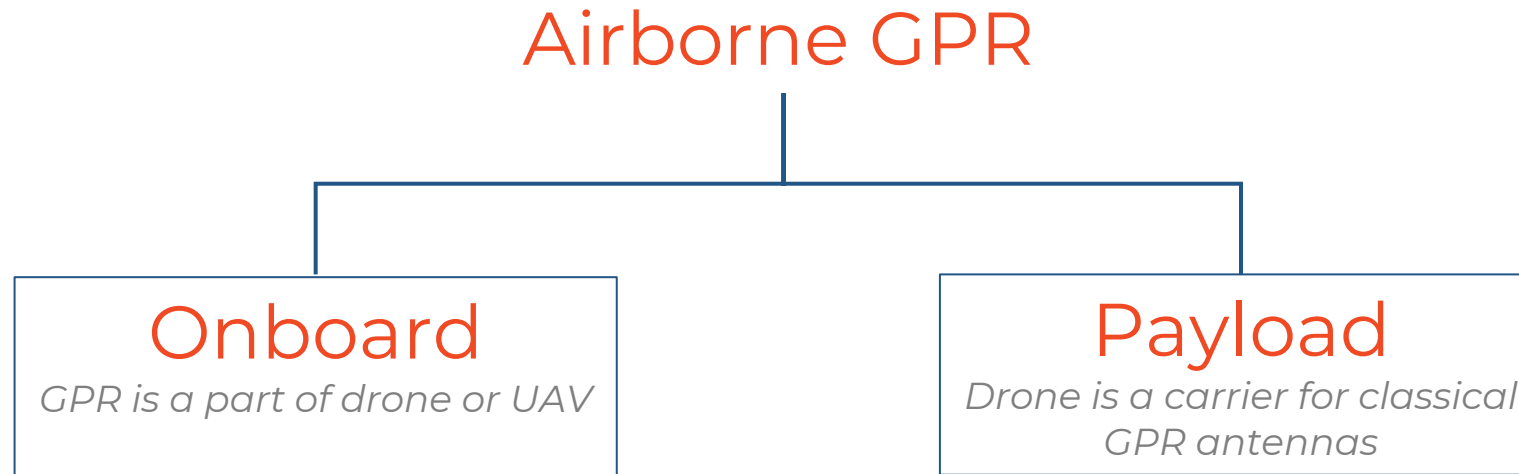
Kotowski, et al., 2022)



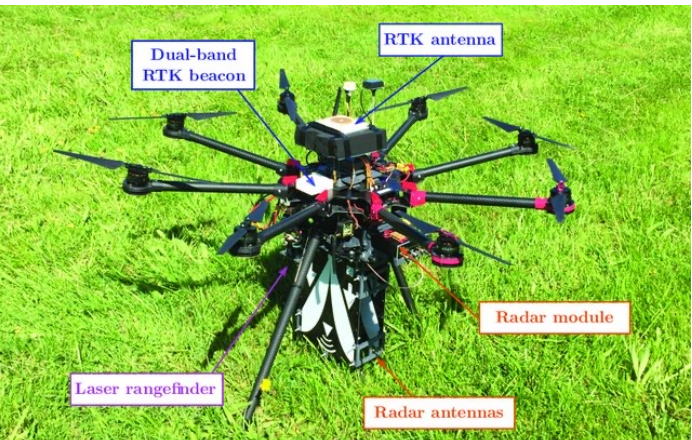
Review

An Overview on Down-Looking UAV-Based GPR Systems

Carlo Noviello ^{1,*} , Gianluca Gennarelli ¹, Giuseppe Esposito ^{1,2} , Giovanni Ludeno ¹ , Giancarmine Fasano ² ,
Luigi Capozzoli ³ , Francesco Soldovieri ¹  and Ilaria Catapano ¹ 



Garcia-Fernandes, et al., (2019)



$f_{min} = 600 \text{ MHz}$
 $f_{max} = 3 \text{ GHz}$

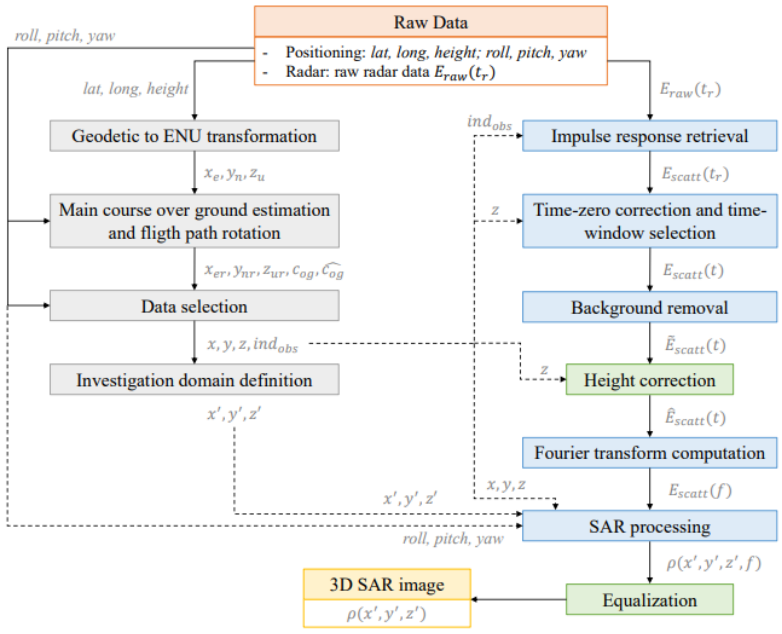
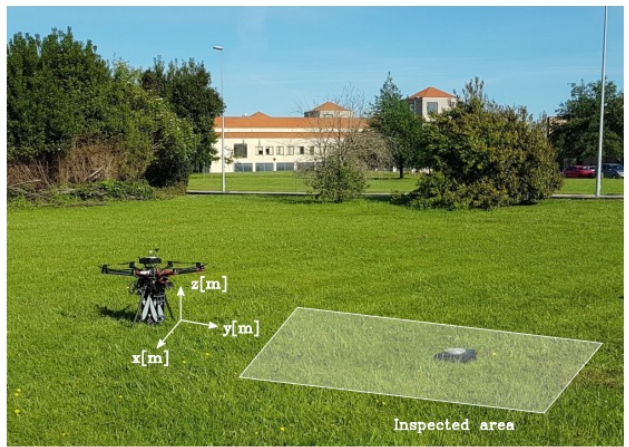


Figure 2. Flowchart of the data processing.

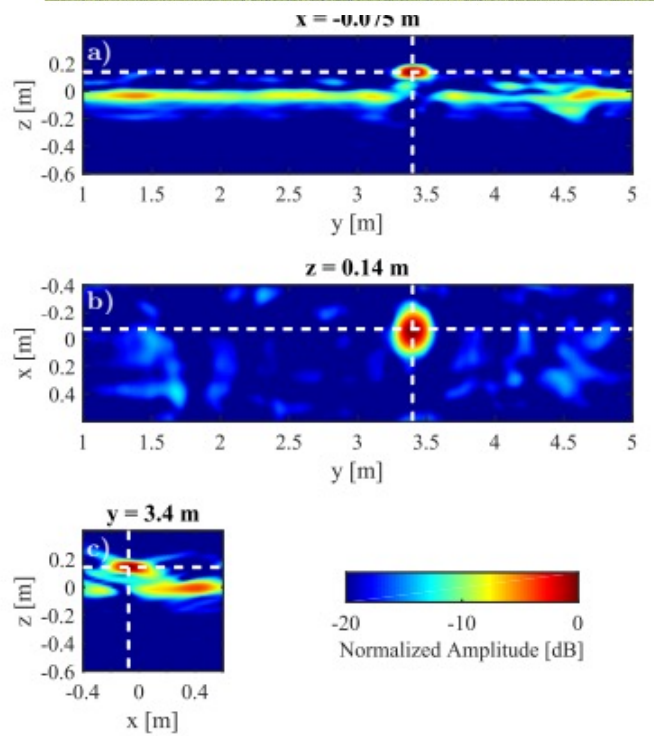




Figure 2. Picture of UAV GPR System 8, Courtesy of Department of Industrial Engineering (DII) of University of Naples, "Federico II".



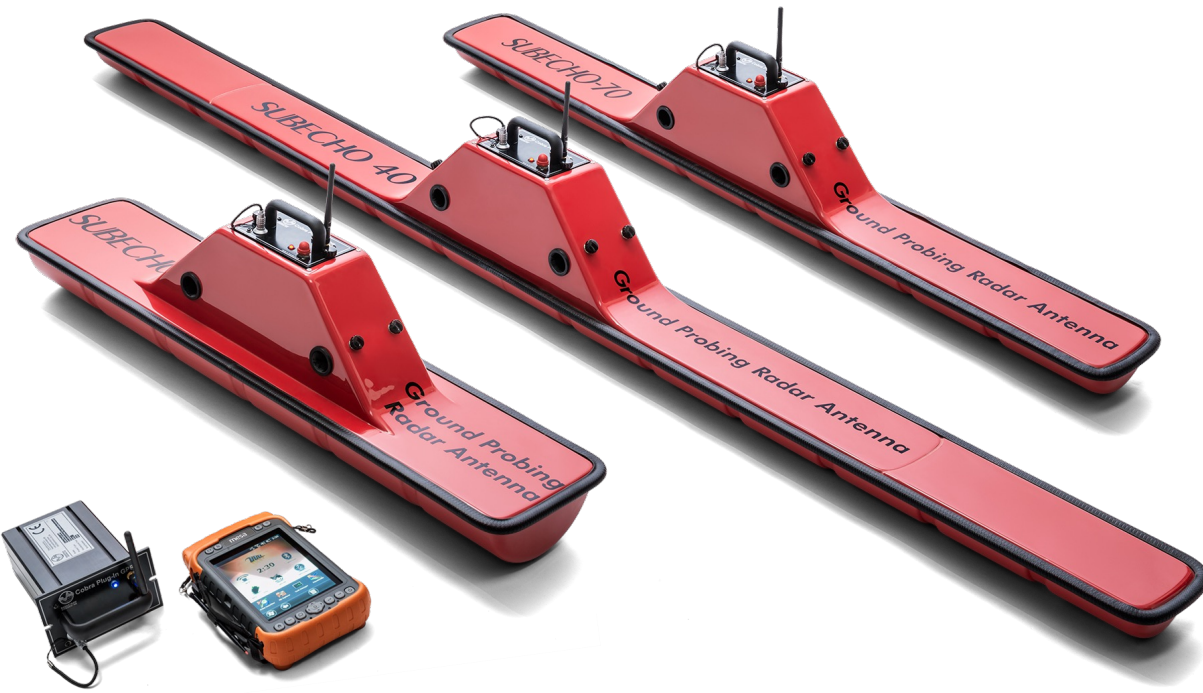
Figure 3. Picture of UAV GPR System 9. Courtesy of Deutsches Zentrum für Luft- und Raumfahrt (DLR), Germany.

Noviello, et al., (2022)

Table 1. UAV GPR systems.

System	Radar Technology	Frequency Range	Antenna	Measurement Configurations	UAV Platform
System 1 [3]	FMCW	Ka band	Linear array	MIMO	Small airplane
System 2 [4]	Pulsed Pulson P410	3.1–5.3 GHz	Helix	Bistatic (quasi-monostatic)	DJI Phantom 2
System 3 [5]	Software-defined radio	Carrier frequency: 2 GHz (bandwidth not specified)	Antipodal Vivaldi antennas	Bistatic configuration with a 45° deg inclination	Hexacopter
System 4 [6]	Stepped frequency	1–4 GHz	Horn	Bistatic (quasi-monostatic)	DJI Matrice 600 Pro
System 5 [8]	M-Sequence UWB radar sensor	System bandwidth: 5.05 GHz (0.95–6 GHz)	1 TX custom designed spiral + 2 RX Vivaldi antennas	Two Vivaldi	'Kraken' octocopter
System 6 [9]	Pulsed Pulson P410	Frequency band: 3.1–5.1 GHz	Helix antennas	Quasi-monostatic	DJI Spreading Wings S1000+
System 7 [10]	M-sequence UWB radar	100 MHz–6 GHz	Two UWB Vivaldi antennas or two log-periodic antennas	Quasi-monostatic	DJI Spreading Wings S1000+
System 8 [11]	Pulsed Pulson P440	Frequency bandwidth: 3.1–4.8 GHz Carrier frequency: 3.95 GHz	Two log-periodic PCB antennas (Ramsey LPY26)	Quasi-monostatic configuration: down-looking	Self-assembled DJI F550 hexacopter
System 9 [15]	FMCW	0.5–3 GHz	Vivaldi patch antennas	Bistatic (quasi-monostatic)	DJI Matrice 600 Pro
System 10 [16]	SFCW Planar R60 VNA	Selected frequency step: 10 MHz Selected frequency bandwidth: 500–700 MHz	Hybrid horn-dipole antenna transmitting and receiving, combining a tapered TEM horn and a half-wave dipole	Monostatic stepped-frequency continuous wave (SFCW)	X8 model made of 8 motors and 4 arms (2 motors per arm) from RCTakeOff
System 11 [17]	SFCW	0.55–2.7 GHz	Hybrid Vivaldi-Horn antenna	Bistatic (quasi-monostatic)	DJI Matrice 600 Pro
System 12 [18]	Pulsed Cobra Plug-In GPR	0.5–260 MHz	COBRA Plug-in SE-150	Monostatic	DJI Matrice 600 Pro
System 13 [19]	Pulsed Cobra Plug-In GPR Cobra CBD Zond-12e	0.5–1000 MHz	COBRA Plug-in SE-70 COBRA Plug-in SE-150 Cobra CBD 200/400/800	Monostatic	DJI Matrice 600 DJI Matrice 600 Pro
System 14 [23]	Pulsed K2 IDS radar	Carrier frequency: 900 MHz (bandwidth not specified)	Not specified	Monostatic	Venture VFF_H01

Noviello, et al., (2022)



<http://www.radarteam.se/>

	GPS Integrated real-time SBAS with 2-5 m typical accuracy		
COBRA PLUG-IN ANTENNAS SUBECHO MODELS	Model SE-40	Model SE-70	Model SE-150
BW [10 dB], Bandwidth [MHz]	15-105 [90 MHz]	20-140 [120 MHz]	20-280 [260 MHz]
Center frequency @ $\xi_r=9$ [MHz]	52	80	124
BW/CF-ratio [%]	173	150	210
Vertical resolution @ $\xi_r=9$ [$\lambda/4$]	48 cm	31 cm	21 cm
Horizontal resolution @ depth= λ	141 cm	88 cm	59 cm
Size [L x W x H]	200 x 15 x 21 cm	139 x 15 x 21 cm	92 x 22 x 22 cm
Weight [kg]	4.7	3.7	3.5

MALÅ GeoDrone 80 Features

- Using our unique MALÅ HDR GPR technology
- Support all standard drones with adequate lift power (>3,5 kg)
- Optimized for specific critical application areas
- Wireless real-time monitoring compatible with other MALÅ GX solutions
- Suitable for automated drone surveying

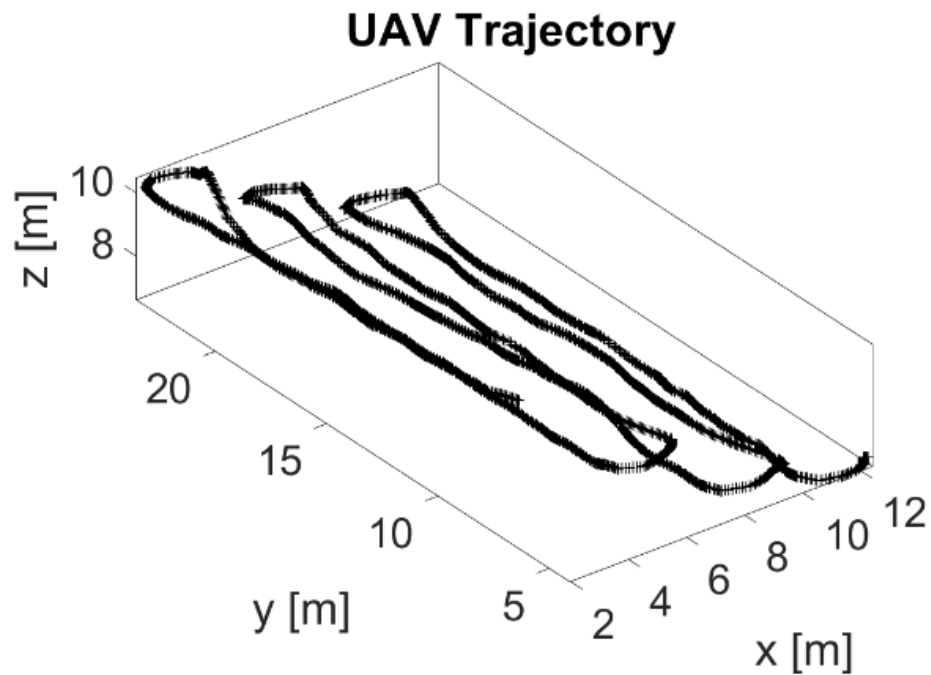
Technical Specification

Core Technology:	MALÅ HDR GPR
Dimension excl. drone:	W580 x L1040 x H240 mm (W23" x L41" x H9½")
Antenna separation:	530 mm (21")
Antenna weight incl. 2 batteries:	3.23 kg (7 lb 2 oz)
Antenna weight excl. 2 batteries:	2.31 kg (5 lb 1 oz)
Battery weight:	0.46 kg (1 lb)
Operating time:	Up to 1 hour
Antenna Frequencies:	80 MHz
Communication:	Complies with IEEE802.11 b/g/n
Built-in positioning:	DGPS (SBAS)

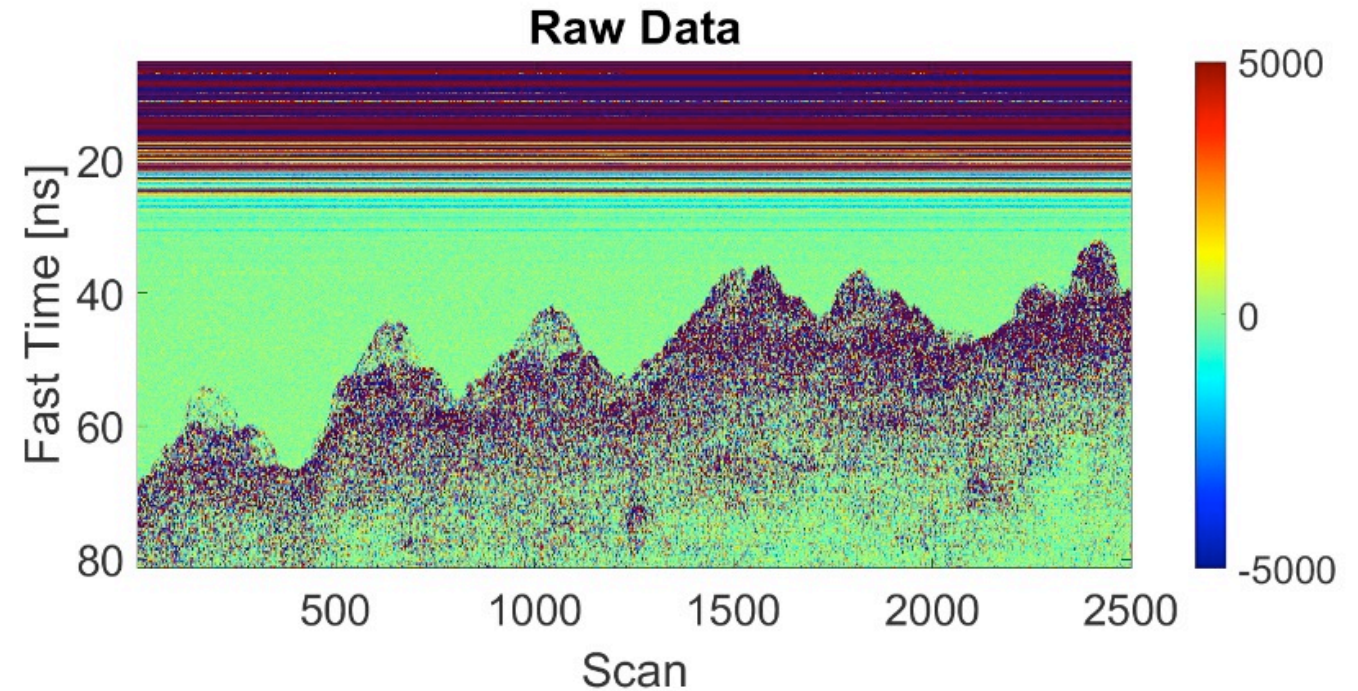
Responsibility & liability

The purchaser must investigate and adhere to the current laws, regulations (e.g. ETSI, FCC) and any required permissions related to the use of airborne GPR in the relevant location of use. Guideline Geo accepts no responsibility nor liability in regards to the above.





Flight Dynamics
(speed/altitude/stability)



Flight height /clutter effects /air soil reflections

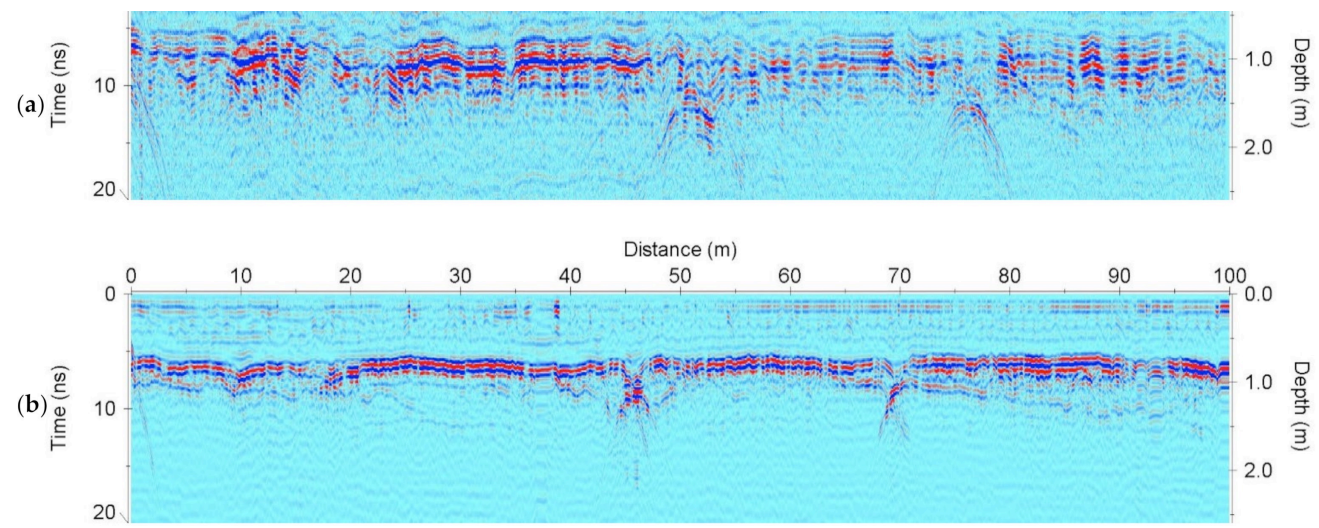
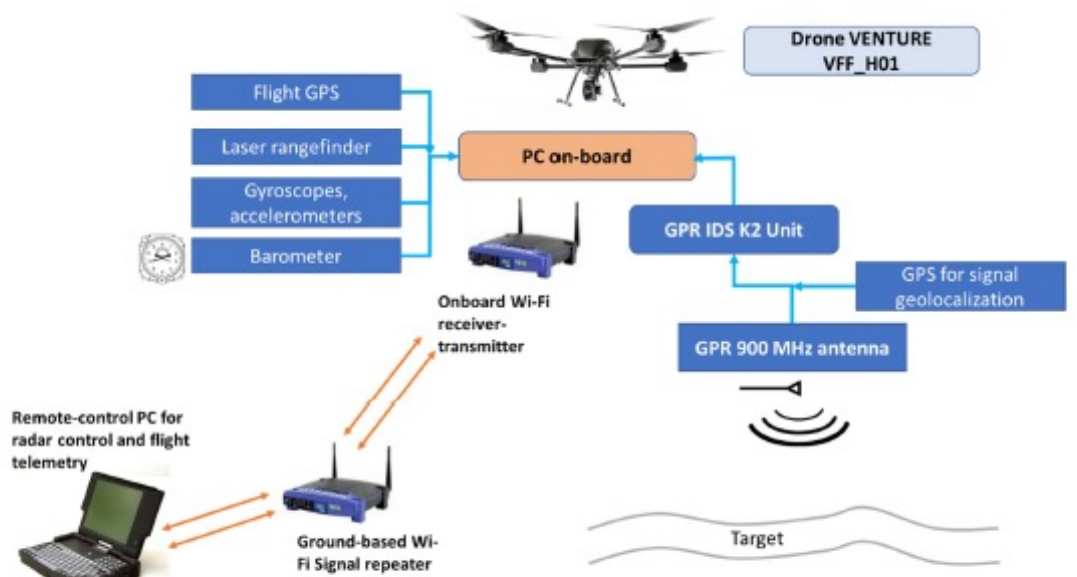
[Noviello, et al., \(2022\)](#)

Article Drone-Borne Ground-Penetrating Radar for Snow Cover Mapping

Andrea Vergnano *¹, Diego Franco and Alberto Godio



Figure 2. The drone deployed in the Cheneil survey area.



Drone radar: A new survey approach for Archaeological Prospection?

Roland Linck¹, Alen Kaltak²

¹Bavarian State Department of Monuments and Sites (BLfD), Munich, Germany, ²Drone it GmbH, Munich, Germany



Fig. 1. Drone radar equipment consisting of DJI M600 hexacopter and Drone it GPR antenna (in black cylinder below drone) during survey in *Cambodunum*.

Drone it GmbH - 80MHz

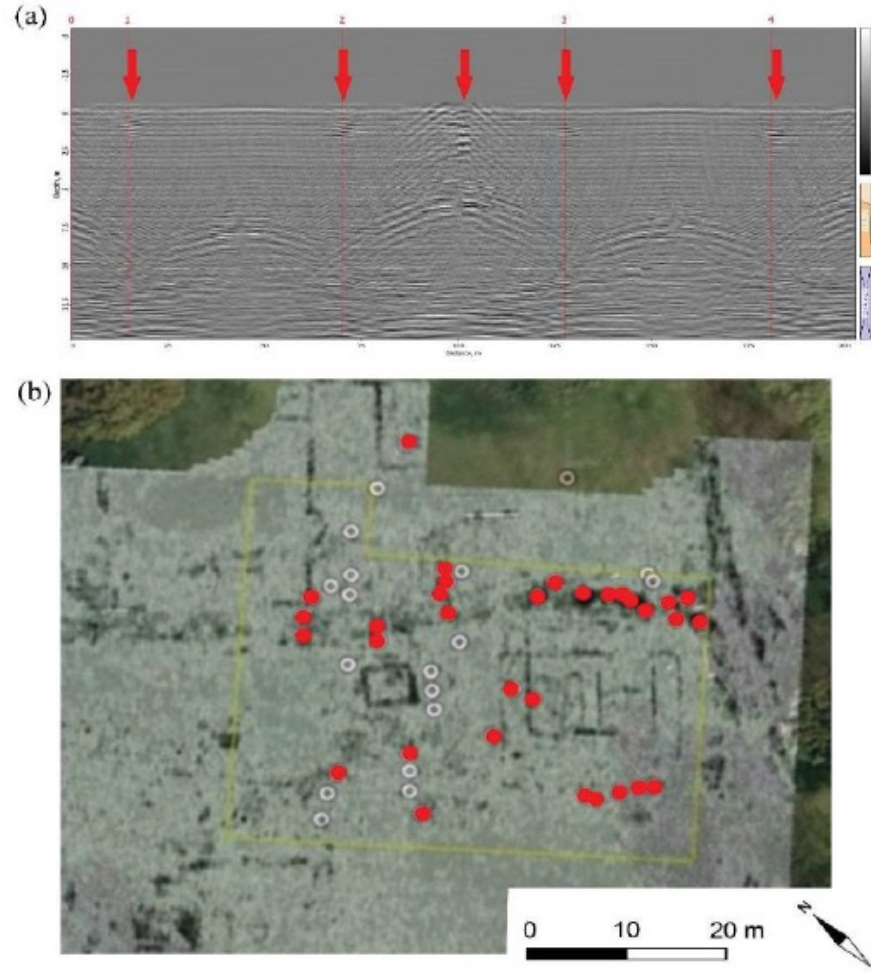
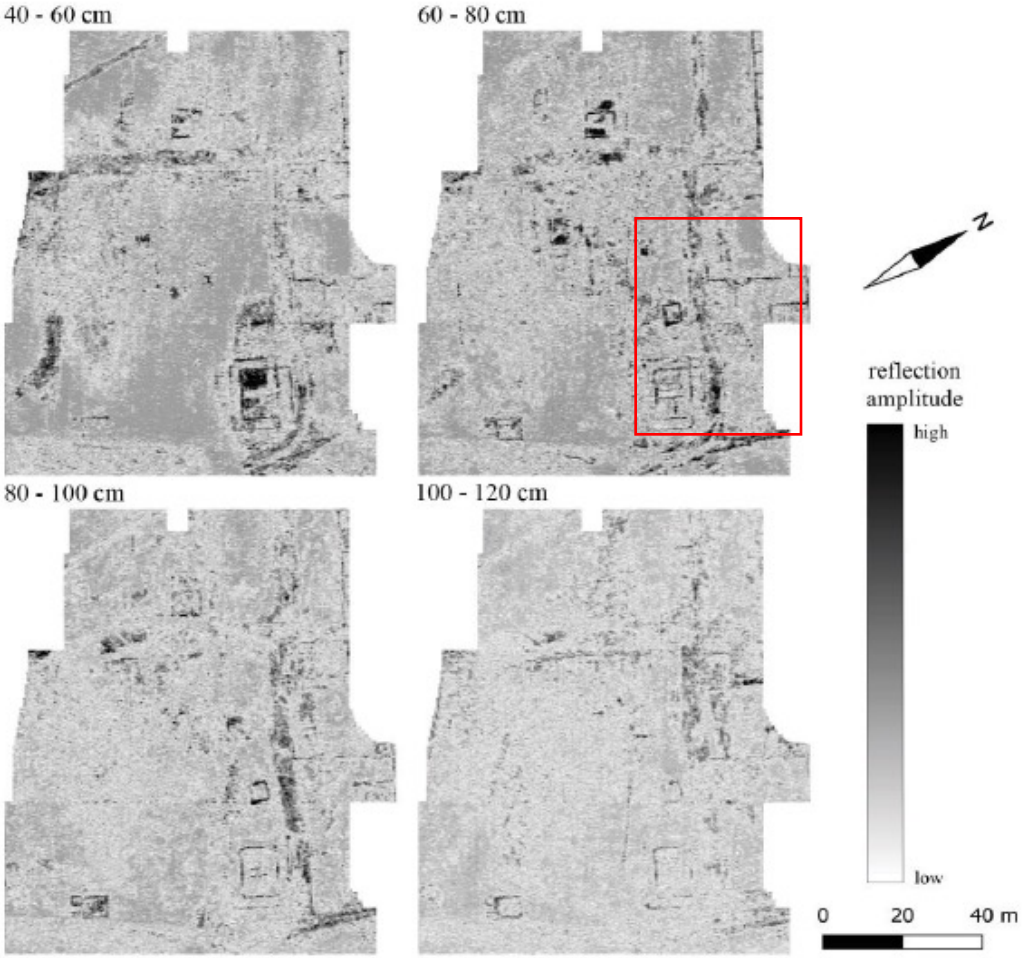


Fig. 2. Selection of depth slices of GPR survey covering the whole Roman forum of *Cambodunum*. GSSI SIR-3000 with 400MHz antenna, sample density: 2cm x 25cm, grid size: 94m x 117m.

Fig. 3. (a) Sample profile of drone radar showing several anomalies at around 1m depth due to buried archaeological remains; relevant anomalies marked with red arrows. (b) Mapping of clear hyperbola apexes onto the 60cm-80cm depth slice of ground-based GPR survey. Red dots mark those hyperbolas fitting quite well to the location of known Roman walls or roads

- **UAV's or and drones are gaining more and more capabilities day by day (Autonomous flights, payload capacity, stabilization, accurate positioning, endurance, etc).**
- Based on the above developments EM sensors/devices are mounted on the vehicles.
- **As of today's situation, these systems seem to be used mostly for searching for near-surface objects (UXO, landmines)and for research in areas covered with snow and ice.**
- High frequency antennae seem to produce better results therefore penetration depth/resolution is not enough for archaeological prospecting yet.



YETI



Figure 2. Polar rover *Yeti* during operations in the McMurdo shear zone, Antarctica, in 2010. *Yeti* towed the same 400 MHz GPR antenna (located in an inner tube) as pushed ahead of the Pisten Bully manual GPR vehicle (seen in the background). Note the low wheel sinkage, typical for the 81 kg rover on natural polar snowfields.

Lever, et al., (2012)

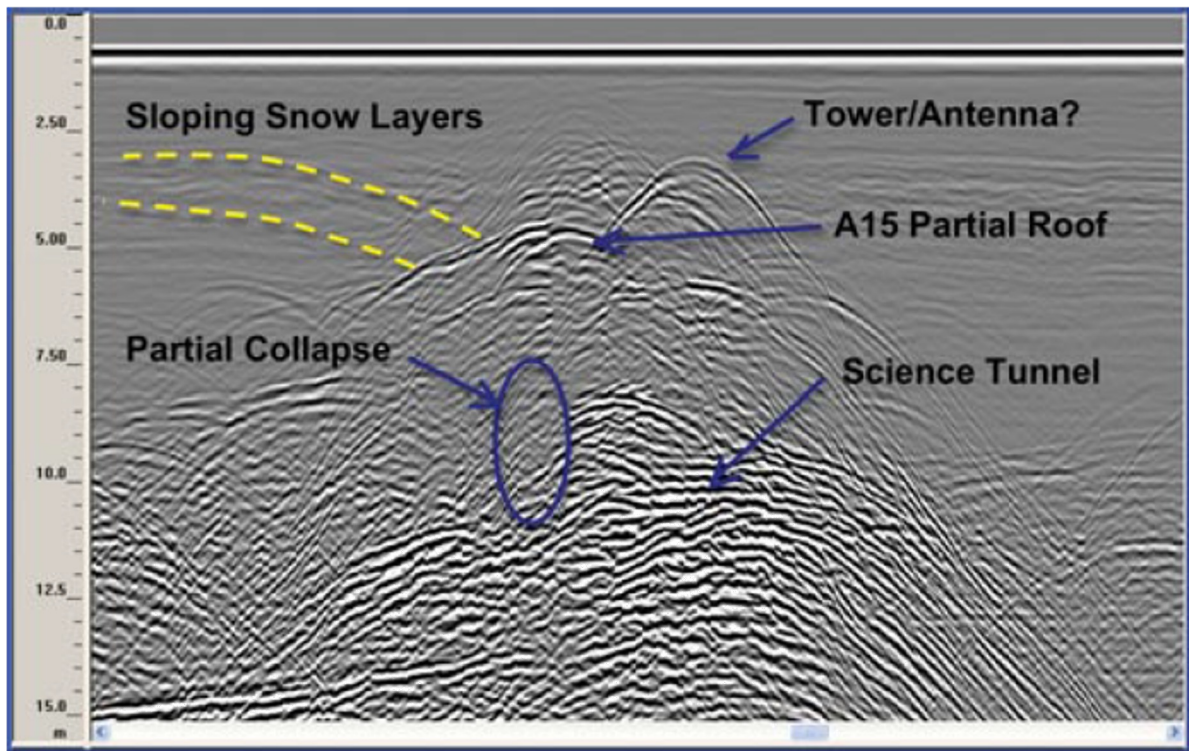
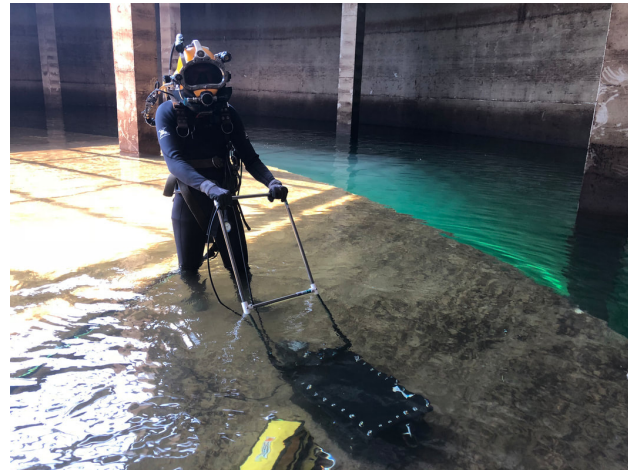
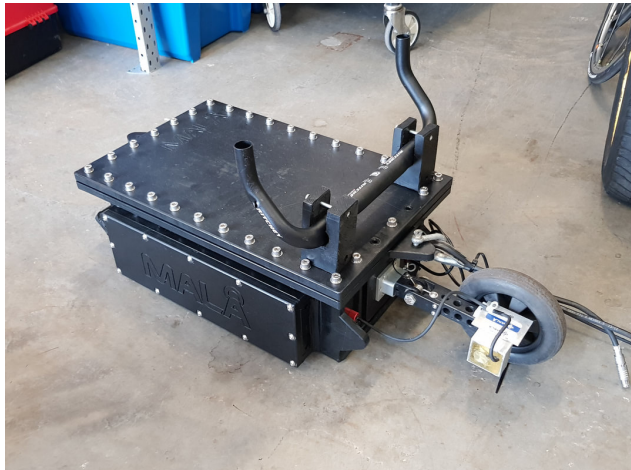


Figure 13. Radargram along eastern boundary of Old Pole showing partially collapsed buildings and science tunnel identified also in 2010 manual survey. Building A15 was collapsed with machinery in late December 2011.



Ruffell ve Parker (2021)

Critical issues:
Water column height
Conductivity of water



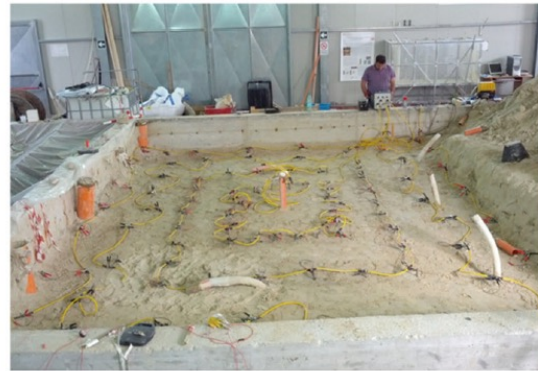
<https://www.malagpr.com.au/underwater-gpr.html>

ERT and GPR Prospecting Applied to Unsaturated and Subwater Analogue Archaeological Site in a Full Scale Laboratory

Luigi Capozzoli ¹, Valeria Giampaolo ¹, Gregory De Martino ¹, Felice Perciante ¹, Vincenzo Lapenna ¹ and Enzo Rizzo ^{1,2,*}



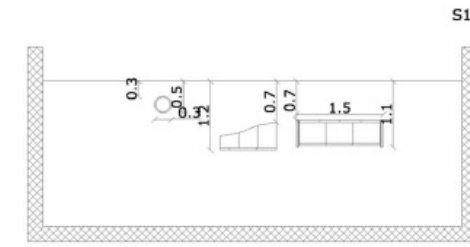
(a)



(b)



(a)



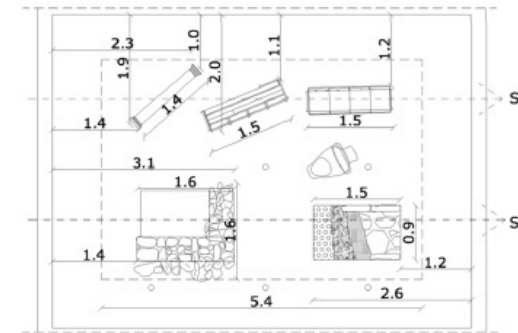
(c)



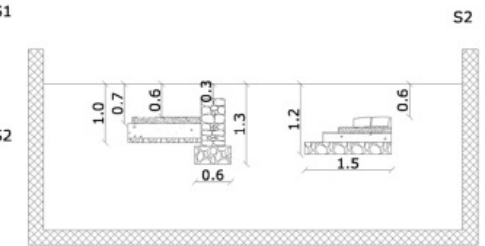
(c)



(d)



(b)



(d)

Figure 2. The archaeological framework reconstructed in the laboratory: (a) plan of remains (b) and transversal sections S1 (c) and S2 (d). The circles shown in the maps represent the positions of the piezometers and the numbers indicate the distance in meters. The pool is 12 m × 7 m × 3 m.

ERT and GPR Prospecting Applied to Unsaturated and Subwater Analogue Archaeological Site in a Full Scale Laboratory

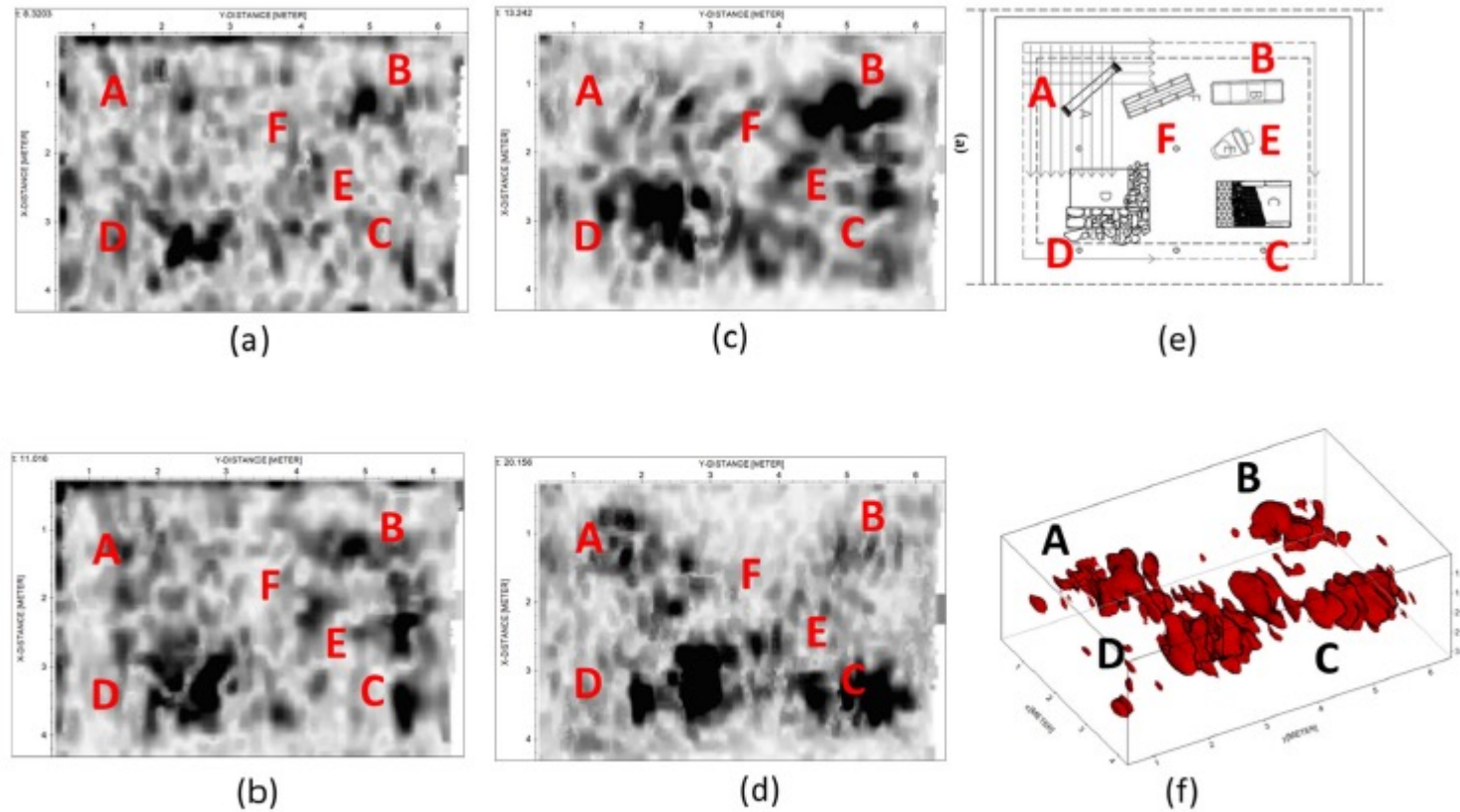


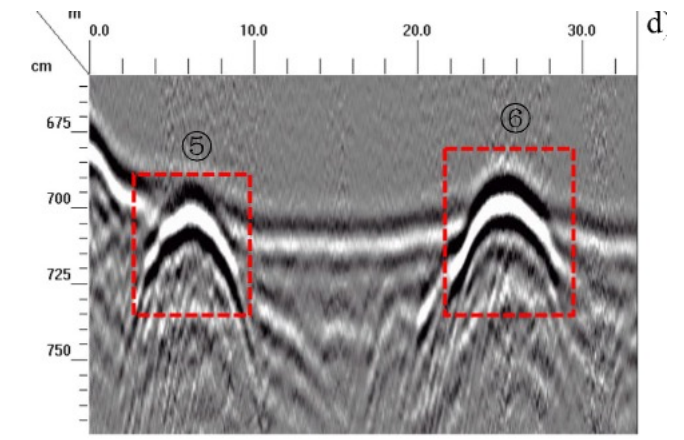
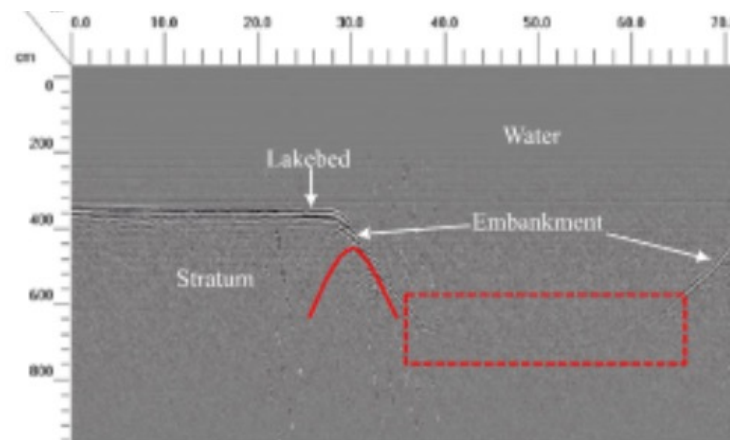
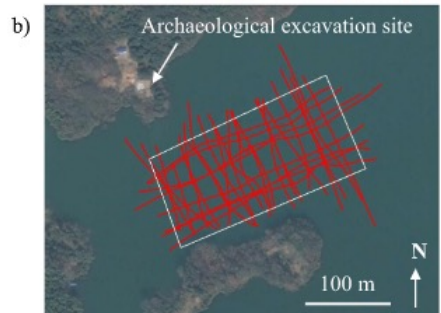
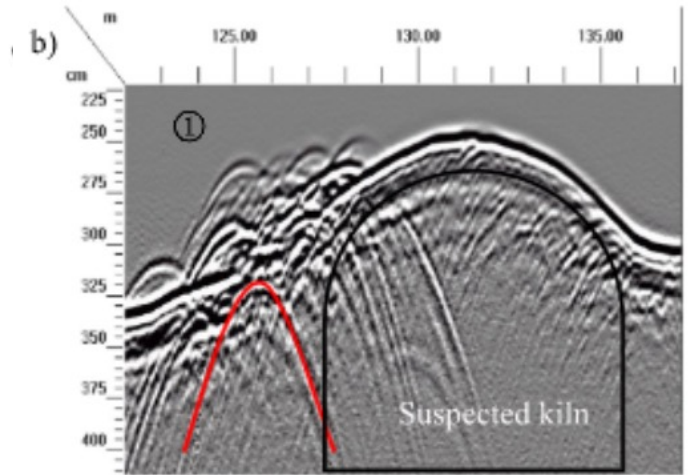
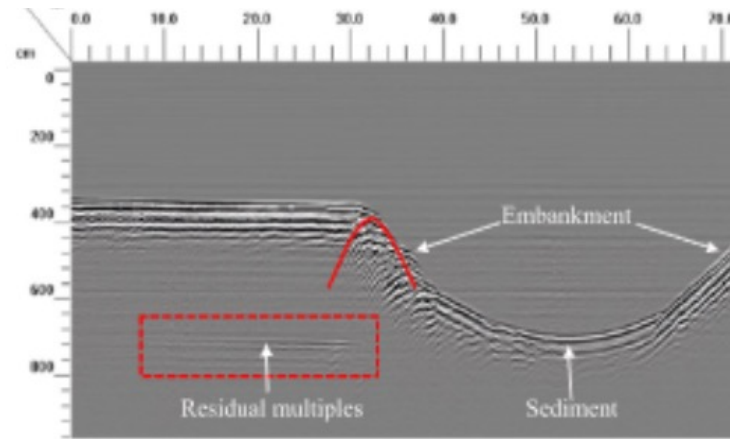
Figure 6. Time-slices at the depths of 0.25 m (a), 0.45 m (b), 0.70 m, and (c) 1.00 m (d) with a water table at a depth of 1.50 m (WL3). In (f) the 3D iso-amplitude volumes obtained selecting only the highest reflections: (e) the plane of the test site.

Underwater archaeological investigation using ground penetrating radar: A case analysis of Shanglinhu Yue Kiln sites (China)

Tan Qin^a, Yonghui Zhao^{a,*}, Guocong Lin^b, Shufan Hu^a, Cong An^a, Dexiang Geng^a, Chunfeng Rao^a

^a School of Ocean & Earth Science, Tongji University, No.1239 Siping road, 200092 Shanghai, China

^b Ningbo Municipal Institute of Cultural Relics and Archaeology, No.203 Lantian Road, 315012 Zhejiang, China



- **Although there exist other EM methods such as VLF/HLEM/TDR GPR is dominated the near surface investigations due to recent developments and its superiority about 3S (Speed-Sensitivity-Spatial Resolution)**
- Numerous examples of the GPR method can be found in the literature about the investigation of archaeological sites.
- **Because of the success of the method on imaging near surface in 2D and 3D, further developments achieved as multichannel instrumentation, UAV or drone-based systems. Latter is still under development.**
- Process of the GPR data reached to a standard but there are still developments in visualization, handling large size data volumes, image/volume rendering etc.
- **UAV based EM systems are useful for detecting UXO, snow layer thickness but not archaeological features yet. But UGV's are good solutions for ground autonomous GPR measurements.**
- Unwater/water level measurements at fresh water environments produce good results depending on the water column height and resistivity of water.

- Aitken, M.J. (1974). *Physics and archaeology*, 2nd edition. Oxford: Clarendon Press, 286 pp.
- Aitken, M.J., Webster, G., and Rees, A. (1958). Magnetic prospecting: *Antiquity* 32, 270-271.
- Al-Saadi, OS, Schmidt, V, Becken, M, Fritsch, T. Very-high-resolution electrical resistivity imaging of buried foundations of a Roman villa near Nonnweiler, Germany. *Archaeological Prospection*. 2018; 25: 209– 218. <https://doi.org/10.1002/arp.1703>
- Annan, A.P., 2009. Electromagnetic Principles of Ground Penetrating Radar. In *Ground Penetrating Radar: Theory and Applications*, edited by Harry M. Jol, pp. 3-40. Elsevier, Amsterdam.
- Berard, B. A., & Maillol, J. M. (2008). Common- and multi-offset ground-penetrating radar study of a Roman villa, Tourega, Portugal. *Archaeological Prospection*, 15(1), 32–46.
- Booth, A. D., Linford, N. T., Clark, R. A., & Murray, T (2008). Three-dimensional, multi-offset ground-penetrating radar imaging of archaeological targets. *Archaeological Prospection*, 15(2), 93–112.
- Campana, S. Piro, S. Felici, C. and Ghisleni M. 2006. From space to place: The Aiali Project (Tuscany Italy) *Bar International Series*, 1568, 131.
- Capozzoli L, Giampaolo V, De Martino G, Perciante F, Lapenna V, Rizzo E. ERT and GPR Prospecting Applied to Unsaturated and Subwater Analogue Archaeological Site in a Full Scale Laboratory. *Applied Sciences*. 2022; 12(3):1126. <https://doi.org/10.3390/app12031126>
- Chamola, V. Kotes, P., Agarwal , A. N., Gupta, N. And Guizani A. 2021. A Comprehensive Review of Unmanned Aerial Vehicle Attacks and Neutralization Techniques, *Ad Hoc Networks*, Volume 111, 102324.
- Conyers, L. (2013). *Ground-penetrating radar for archaeology*. Lanham, MD: Rowman and Littlefield Publishers, AltaMira Press.
- Dong, Y. And Ansari, F. 2011. Non-destructive testing and evaluation (NDT/NDE) of civil structures rehabilitated using fiber reinforced polymer (FRP) composites In *Woodhead Publishing Series in Civil and Structural Engineering, Service Life Estimation and Extension of Civil Engineering Structures*, p 193-222 <https://doi.org/10.1533/9780857090928.2.193>.
- Gabler M, Trinks I, Nau E, Hinterleitner A, Paasche K, Gustavsen L, Kristiansen M, Tønning C, Schneidhofer P, Kucera M, Neubauer W. 2019. Archaeological Prospection with Motorised Multichannel Ground-Penetrating Radar Arrays on Snow-Covered Areas in Norway. *Remote Sensing*. 2019; 11(21):2485. <https://doi.org/10.3390/rs11212485>

- Gabryś, Marta, and Łukasz Ortyl. 2020. "Georeferencing of Multi-Channel GPR—Accuracy and Efficiency of Mapping of Underground Utility Networks" *Remote Sensing* 12, no. 18: 2945. <https://doi.org/10.3390/rs12182945>
- Gaffney, V, Neubauer, W, Garwood, P, et al. Durrington walls and the Stonehenge Hidden Landscape Project 2010–2016. *Archaeological Prospection*. 2018; 25: 255– 269. <https://doi.org/10.1002/arp.1707>
- Garcia-Fernandez M, Alvarez-Lopez Y, Las Heras F. Autonomous Airborne 3D SAR Imaging System for Subsurface Sensing: UWB-GPR on Board a UAV for Landmine and IED Detection. *Remote Sensing*. 2019; 11(20):2357. <https://doi.org/10.3390/rs11202357>
- Gavazzi, B., Reiller, H. & Munsch, M. (2021). An Integrated Approach for Ground and Drone-Borne Magnetic Surveys and their Interpretation in Archaeological Prospection. *ArcheoSciences*, 45-1, 165-168. <https://doi.org/10.4000/archeosciences.9325>
- Grasmueck, M., Weger, R., & Horstmeyer, H. (2003). How dense is dense enough for a real 3D GPR survey? In Proceedings 2003 SEG Annual Meeting, 26-31 October, Dallas, Texas.
- Grasmueck, M., Weger, R., & Horstmeyer, H. (2005). Full-resolution 3D GPR imaging. *Geophysics*, 70(1), K12–K19.
- Goodman, D. and Piro S. 2013. *GPR Remote Sensing in Archaeology*. Springer, ISBN 978-3-642-31856-6 ISBN 978-3-642-31857-3 (eBook)
- Herbich, T. and Spencer, J. 2008. TELL EL-BALAMUN Geophysical and Archaeological Survey, 2007-2008. https://pcma.uw.edu.pl/wp-content/uploads/pam/PAM_2007_XIX/131-141_Tell_el-Balamun.pdf
- Khalil, M., Ali, A., Santos, F., Mesbah, H., Massoud, U. (2010). VLF-EM study for archaeological investigation of the labyrinth mortuary temple complex at Hawara area, Egypt. *Near Surface Geophysics*. 8. 10.3997/1873-0604.2010004.
- Kotowski, P.O.; Becken, M.; Thiede, A.; Schmidt, V.; Schmalzl, J.; Ueding, S.; Klingen, S. Evaluation of a Semi-Airborne Electromagnetic Survey Based on a Multicopter Aircraft System. *Geosciences* **2022**, 12, 26. <https://doi.org/10.3390/geosciences12010026>
- Lever, J.H., Delaney, A.J., Ray, L.E., Trautmann, E., Barna, L.A. and Burzynski, A.M. (2013), Autonomous GPR Surveys using the Polar Rover Yeti. *J. Field Robotics*, 30: 194-215. <https://doi.org/10.1002/rob.21445>

- Linck, R. and Kaltak, A. 2019. Drone radar: A new survey approach for Archaeological Prospection? 13th International conference on Archaeological prospection 28 august - 1 september 2019 Sligo – Ireland.
- Noviello C, Gennarelli G, Esposito G, Ludeno G, Fasano G, Capozzoli L, Soldovieri F, Catapano I. An Overview on Down-Looking UAV-Based GPR Systems. *Remote Sensing*. 2022; 14(14):3245. <https://doi.org/10.3390/rs14143245>
- Ruffell, A., & Parker, R. 2021. Water penetrating radar. *Journal of Hydrology*, 597, 126300.
- Sarris, A., Papadopoulos, N., Trigkas, V., Lolos, Y., and Kokkinou E. 2007. Recovering the Urban Network of Ancient Sikyon Through Multi-component Geophysical Approaches. CAA Berlin, April,2-6, 2007.
- Stoll, J.B, Noellenburg, R., Becken, M., Tezkan, B. Yogeshwar, P. Bergers, R. 2019. Semi-Airborne electromagnetics using a multicopter. GEM 2019 Xi'an: International Workshop on Gravity, Electrical & Magnetic Methods and Their Applications Xi'an, China, May 19–22, 2019
- Swinbourne, M., Sparrow, E., Hatch, M., Bowden, T. and Taggart D. 2014. Using near-surface geophysics to assist with the management of southern hairy-nosed wombats (*Lasiorhinus latifrons*) in South Australia *The Leading Edge* 33:12, 1356-1362
- Trinks, I., Neubauer, W., Doneus, M. (2012). Prospecting Archaeological Landscapes. In: Ioannides, M., Fritsch, D., Leissner, J., Davies, R., Remondino, F., Caffo, R. (eds) *Progress in Cultural Heritage Preservation. EuroMed 2012. Lecture Notes in Computer Science*, vol 7616. Springer, Berlin, Heidelberg. https://doi.org/10.1007/978-3-642-34234-9_3
- Trinks I., Hinterleitner A., Neubauer W., Nau E., Löcker K., et al. 2018. Large-area high-resolution ground-penetrating radar measurements for archaeological prospection. *Archaeological Prospection*, 25 (3), pp. 171 – 195.
- Vergnano A, Franco D, Godio A. Drone-Borne Ground-Penetrating Radar for Snow Cover Mapping. *Remote Sensing*. 2022; 14(7):1763. <https://doi.org/10.3390/rs14071763>
- Wells, J.2020. https://www.researchgate.net/publication/343547315_Archaeological_Aerial_Thermography_and_Near_Infrared_Photography accessed: 06, Sept, 2022.